CANARY-1B-V2 & PARAKEET-TDT-0.6B-V3: EFFICIENT AND HIGH-PERFORMANCE MODELS FOR MULTILINGUAL ASR AND AST

**Monica Sekoyan,*[*] Nithin Rao Koluguri,*[*] Nune Tadevosyan*[*]
Piotr Zelasko, Travis Bartley, Nick Karpov, Jagadeesh Balam, Boris Ginsburg
NVIDIA
Santa Clara, CA 95051, USA
{msekoyan, nkoluguri, ntadevosyan}@nvidia.com

ABSTRACT

This report introduces **Canary-1B-v2**[1], a fast, robust multilingual model for Automatic Speech Recognition (ASR) and Speech-to-Text Translation (AST). Built with a FastConformer encoder and Transformer decoder, it supports 25 European languages. The model was trained on 1.7M hours of total data samples, including Granary and NeMo ASR Set 3.0, with non-speech audio added to reduce hallucinations for ASR and AST. We describe its two-stage pre-training and fine-tuning process with dynamic data balancing, as well as experiments with an nGPT encoder. Results show nGPT scales well with massive data, while FastConformer excels after fine-tuning. For timestamps, Canary-1B-v2 uses the NeMo Forced Aligner (NFA) with an auxiliary CTC model, providing reliable segment-level timestamps for ASR and AST. Evaluations show Canary-1B-v2 outperforms Whisper-large-v3 on English ASR while being 10× faster, and delivers competitive multilingual ASR and AST performance against larger models like Seamless-M4T-v2-large and LLM-based systems.

We also release **Parakeet-TDT-0.6B-v3**[2], a successor to v2, offering multilingual ASR across the same 25 languages with just 600M parameters.

1 INTRODUCTION

Modern speech processing systems for Automatic Speech Recognition (ASR) and Speech Translation (ST) are predominantly built on the encoder-decoder paradigm. Architectures such as the TransformerVaswani et al. (2023) have proven highly effective, with models like WhisperRadford et al. (2023) and SeamlessM4TBarrault & Others (2023) demonstrating that training on massive, weakly supervised multilingual datasets can yield state-of-the-art results. Despite their strong performance, these models often require large resources and run slowly, creating a trade-off between accuracy, size, and speed. Specialized architectures like Conformer and its efficient variant, FastConformer, have been developed to better capture speech-specific features with a smaller computation footprint.

This work introduces Canary-1B-v2, a multilingual, multi-task model designed to deliver robust ASR and AST performance with high efficiency. In addition, we release Parakeet-TDT-0.6B-v3, a smaller yet more accurate ASR model supporting the same 25 languages.

The key contributions of this paper are:

- **A Multi-Stage Training and Fine-Tuning Strategy**: A two-stage pre-training regimen followed by a high-quality fine-tuning stage with dynamic weight scheduling to address significant data imbalances in large-scale multilingual corpora.

[*] These authors contributed equally. Listed in alphabetical order based on First Name.

[1] https://huggingface.co/nvidia/canary-1b-v2

[2] https://huggingface.co/nvidia/parakeet-tdt-0.6b-v3

- **Comprehensive Data Curation**: Training on a 1.7 million-hour dataset spanning 25 languages, combining pseudo-labeled and human-annotated data, and incorporating non-speech audio to improve robustness.
- **Efficient Architecture and Timestamp Generation**: Canary-1B-v2 leverages a FastConformer encoder and a unified BPE tokenizer for all languages, delivering high throughput. It integrates the NeMo Forced Aligner (NFA) with an auxiliary CTC model for accurate segment-level timestamps in both ASR and AST tasks.
- **State-of-the-Art Performance**: Canary-1B-v2 achieves competitive or superior results to much larger models on ASR and AST benchmarks, including the Hugging Face Open ASR Leaderboard, while providing significantly faster inference.

This report details the models' architectures, the data curation and balancing strategies, the multi-stage training process, and extensive evaluations against leading speech processing systems.

2 Architecture

Modern speech recognition and speech translation systems are predominantly built on the encoder-decoder paradigm. In this framework, the encoder extracts high-level representations from the raw speech signal, conditioning the decoder to generate text in the target language. The most powerful recent systems employ pure Transformer-based architectures, often trained at a massive speech scale data. For instance, Whisper Radford et al. (2023) demonstrated that training a Transformer encoder-decoder on hundreds of thousands of hours of weakly supervised multilingual data yields state-of-the-art performance on both Automatic Speech Recognition (ASR) and Speech Translation (ST) tasks. Similarly, SeamlessM4T Barrault & Others (2023) extended this approach to create a unified multilingual framework for speech and text translation, underscoring the scalability of Transformer-based designs. Earlier models, such as the Speech-Transformer Dong et al. (2018), were instrumental in establishing the viability of attention-based encoder-decoder architectures for speech processing.

In contrast to general-purpose Transformers, several architectures have been tailored specifically for speech. The Conformer Gulati & Others (2020) augments the Transformer with convolutional modules, enabling it to capture both fine-grained local acoustic patterns and long-range global dependencies. Its optimized variant, the FastConformer Rekesh et al. (2023a), further enhances efficiency through aggressive subsampling and the use of depthwise separable convolutions. Such encoders are often paired with online decoders like the RNN-Transducer (RNN-T) Jain et al. (2019) or Connectionist Temporal Classification (CTC) Graves et al. (2006), which are widely adopted for streaming ASR due to their low-latency characteristics.

For speech translation, however, autoregressive Transformer-based decoders remain dominant, as they excel at modeling cross-lingual dependencies and generating fluent text. Recently, a prominent strategy has been to integrate pre-trained Large Language Models (LLMs) as decoders. This approach leverages the vast linguistic knowledge captured during text-only pre-training and scales effectively across modalities. For example, models like SALMChen et al. (2024a)[3], BESTOW Chen et al. (2024b) and SpeechGPT Zhang et al. (2023) adapt speech encoders to interface with powerful LLMs. One example of such integration is Phi-4-Multimodal Abouelenin et al. (2025). In this architecture, inputs from multiple modalities—including speech—are processed by modality-specific encoders (e.g., a Conformer for speech). The resulting features are projected into a common embedding space via lightweight adapters and then decoded by a shared LLM backbone (Phi-4-Mini) equipped with LoRA adapters for speech-to-text tasks. This design circumvents traditional decoder retraining by adapting the LLM with LoRA, efficiently enabling language generation conditioned on speech inputs.

Notable approach from above models is the Speech-Augmented Language Model (SALM) Chen et al. (2023), which utilizes a frozen pre-trained text LLM and augments it with a speech encoder, a modality adapter, and LoRA layers. This creates a unified architecture for both ASR and ST. Trained with in-context speech instruction tuning, SALM matches the performance of specialized Conformer models while also demonstrating zero-shot adaptation and keyword boosting capabilities. Such designs not only improve translation quality but also align speech models more closely with the architectural principles of today's leading text-based systems.

[3] `https://huggingface.co/nvidia/canary-qwen-2.5b`

2.1 Encoder

In any encoder-decoder architecture for speech, the encoder is a critical component. It is typically responsible for the majority of the model's memory consumption. The full self-attention mechanism in encoder layers often becomes the primary bottleneck during pre-training and inference, especially with long audio sequences. Consequently, the encoder's design plays a central role in determining both the scalability and efficiency of the entire system. Even minor architectural modifications or scaling decisions can yield substantial performance gains. In this work, we focus on the encoder and experiment with two distinct architectures: the FastConformer Rekesh et al. (2023b) and the normalized GPT (nGPT) Loshchilov et al. (2024).

2.1.1 FastConformer

The FastConformer is an evolution of the Conformer encoder, explicitly optimized for computational efficiency in speech tasks. Its primary improvements over the original Conformer include:

- **Aggressive Subsampling (8x):** Input features are downsampled by a factor of 8 at the input stage using convolutional blocks. This significantly shortens the sequence length, reducing computational cost while preserving accuracy.
- **Depthwise Separable Convolutions:** Standard convolutions in both the subsampling layers and the Conformer blocks are replaced with depthwise separable convolutions, which reduces the number of operations while maintaining strong performance.
- **Lightweight Convolutional Modules:** The convolutional kernel size is reduced (e.g., from 31 to 9) and channel dimensions are scaled down, further streamlining the encoder without degrading recognition quality.

These optimizations yield a model that is significantly faster (2–3× inference speedup) and more memory-efficient, while achieving accuracy comparable to or better than the original Conformer.

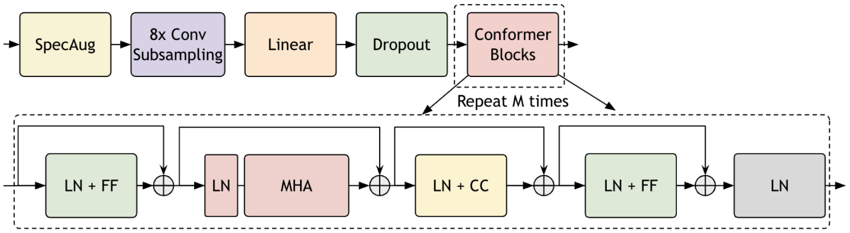

Figure 1: Overview of the **FastConformer** architecture. The input features are first subsampled to a resolution of 80 ms, followed by a linear projection and dropout for dimensionality reduction and regularization. The core of the model consists of a stack of repeated Conformer blocks, each containing four main components: Layer Normalization (LN), a Feed-Forward (FF) module, a Multi-Head Attention (MHA) mechanism, and a Convolutional Module (CC).

2.1.2 nGPT

While the FastConformer optimizes a speech-specific architecture, a different line of research has focused on fundamentally rethinking the Transformer itself. Normalized GPT (nGPT) model Loshchilov et al. (2024) introduces a hyperspherical normalization scheme that constrains all embeddings to a unit hypersphere. This design stabilizes training, improves generalization, and accelerates convergence, enabling the model to reach target validation metrics in fewer steps than standard Transformers.

Building on these ideas, we adapt nGPT into a full encoder-decoder architecture for speech. To the best of our knowledge, this is the first work to explore the nGPT architecture for speech processing tasks. As an initial step, we developed and evaluated an nGPT-based encoder, allowing us to isolate and study its effectiveness in the acoustic domain. For the decoder, we retained a conventional Transformer architecture to ensure that any observed improvements could be directly attributed to the novel encoder design.

Our implementation of the `NGPTEncoder` begins with a Linear subsampling front-end to reduce the temporal resolution of the input spectrogram. The encoder is then constructed as a stack of nGPT layers, with the following key components:

- **Multi-head Attention with Rotary Embeddings.** The attention layers use Rotary Positional Embeddings (RoPE) for long-sequence generalization and standard scaled dot-product attention.
- **Feed-forward Network.** Each layer uses a gated two-stage feed-forward module with a SiLU activation.
- **Hyperspherical Normalization.** All embeddings and intermediate activations are constrained to lie on a unit hypersphere. Query, key, and projection weights are explicitly normalized, with learnable scaling factors (α, σ) regulating the residual contributions from the attention and feed-forward modules.
- **Residual Connections.** Residual paths can be interpreted as a first-order optimization step, where each layer refines the representation by adding an incremental update to the current state.

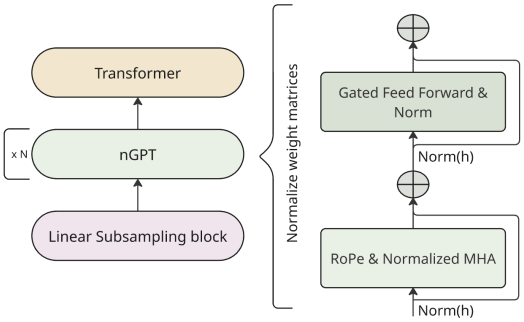

Figure 2: Overview of the nGPT architecture. The input features are first processed by a linear subsampling block. This is followed by a stack of repeated nGPT layers and a Transformer decoder. Each nGPT layer adopts a Transformer-style design with Rotary Position Embeddings (RoPE), multi-head attention, and gated feed-forward modules. Normalization is applied across the embedding dimension, and both activations and weight matrices are normalized, with weight normalization additionally enforced after each optimizer update.

2.1.3 Positional Encodings

Our initial nGPT implementation adopted Rotary Positional Encodings (RoPE) Su et al. (2021) as the baseline. RoPE injects position information by applying a rotation to the query and key vectors, a design known to generalize well in long-context settings. While functional, our experiments with RoPE revealed performance degradation in very long-context ASR and ST scenarios.

To address this limitation, we explored Attention with Linear Biases (ALiBi) Press et al. (2022). ALiBi was originally designed for autoregressive language models, where it adds a static, position-dependent bias to the attention scores, penalizing attention to distant tokens. Since our encoder processes the full context (i.e., it is bidirectional), we modified the original ALiBi formulation to use a symmetric bias matrix, ensuring that both left and right contexts are treated equally. This adaptation allowed us to integrate ALiBi into our nGPT encoder as an alternative positional encoding scheme. This represents the first exploration of ALiBi positional embeddings for speech recognition and translation tasks.

3 Data

Web-scale training data has proven transformative for multi-task and multi-lingual speech systems, delivering substantial performance improvements. However, the scale that enables these gains often

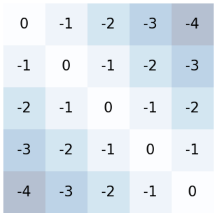

0	-1	-2	-3	-4
-1	0	-1	-2	-3
-2	-1	0	-1	-2
-3	-2	-1	0	-1
-4	-3	-2	-1	0

Figure 3: Symmetric ALiBi bias matrix used in the nGPT encoder. Unlike the original causal ALiBi, which penalizes only future positions, this non-causal variant applies equal bias to tokens before and after the current position, ensuring balanced treatment of left and right context.

comes with quality trade-offs that require careful management. For Canary-1B-v2 and Parakeet-TDT-0.6B-v3, we addressed the data problem from multiple complementary perspectives: task and language balancing, optimal mixing of pseudo-labeled and human-annotated data, and careful curation strategies to maximize data utility while mitigating quality concerns.

In this section, we present all the datasets that comprise our 1.7M hours of training data used to train both models, provide insights into data composition and future balancing decisions, and detail the evaluation datasets used to assess model performance.

3.1 Training Data Curation and Sources

The training data of *Canary-1B-v2* is heavily based on Granary multilingual and multitask dataset Koluguri et al. (2025) which is a super set of three main corpora: MOSELGaido et al. (2024), YTCPleias (2025), and YODASLi et al. (2024), comprising around 0.7 million hours of ASR speech data samples in 25 supported languages, which is pseudo-labeled and translated to other languages for AST tasks with Granary pipeline. Its multi-task speech data components, proven quality of the data processing pipeline, and broad language coverage made it possible to train a model of this scale and scope. However, because much of the data was pseudo-labeled, we also needed to mitigate potential issues that could arise from the limited amount of human-labeled data.

To address this challenge, we augmented Granary with 227,000 hours of high-quality human-labeled data from NeMo ASR Set 3.0, covering all three tasks (ASR, AST X→En, and En→X) across all 25 languages. While representing only 13% of our total training dataset, NeMo ASR Set provides invaluable human-annotated data sourced from proven quality datasets including AMI Kraaij et al. (2005), FLEURS Conneau et al. (2022), Common Voice Ardila et al. (2020), Multilingual LibriSpeech (MLS) Pratap et al. (2020), and language-specific datasets such as Golos Karpov et al. (2021) for Russian.

Another crucial addition to the Granary dataset was a supplementary dataset specifically for the En→X translation task, since Granary originally provided data only for ASR and X→En tasks. This supplementary mono-task dataset was constructed by sampling a subset of the Granary English corpus and generating translations into multiple target languages using the methodology described in Koluguri et al. (2025). In total, it comprised around 480,000 hours of English-to-non-English audio–transcription pairs.

Figure 4 summarizes the distribution of tasks across corpora in our training data. As can be observed, there is a task imbalance present in the training set, where ASR and En→X tasks dominate the dataset, while X→En translation data is comparatively limited. This is a common phenomenon in multi-task training setups, for which we have applied mitigating methods described in Section 4.

For our second model, *Parakeet-TDT-0.6B-v3*, we trained exclusively on the ASR subset of the *Canary-1B-v2* training set (∼660,000 hours across the same 25 languages).

3.2 Non-speech Data for Robustness

To enhance model robustness against hallucinations, particularly those potentially inherited from Whisper-based pseudo-labeling, we incorporated 36,000 hours of non-speech audio into our training

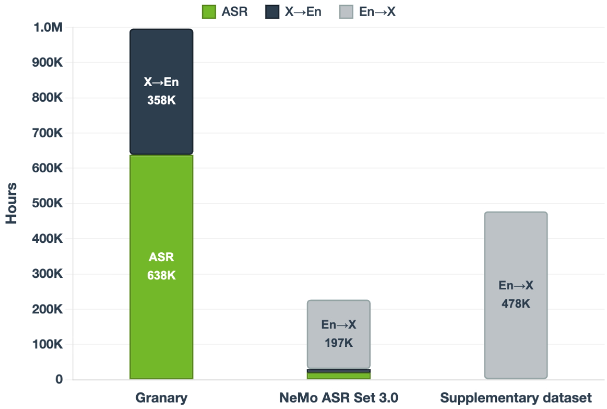

Figure 4: Overview of participating corpora in the training set with within-corpus task divisions.

dataset. These samples, extracted during Granary pipeline filtration steps[4], are paired with empty string targets to teach the model when not to generate transcriptions.

We randomly assigned source-target language pairs to non-speech samples, creating coverage across all possible task combinations (X→X, En→X, and X→En). This approach ensures the model learns to detect and appropriately handle non-speech content regardless of the specified language pair.

With this final addition, we have around 1.7M hours of combined ASR and AST data. For a more detailed overview of the training data decomposition, refer to Appendix 7.

3.3 Language Coverage and Imbalance Analysis

Our training dataset encompasses all 25 target European languages, with Granary serving as the primary source for low-resource languages such as Latvian (lv), Maltese (mt), and Lithuanian (lt). Through VoxPopuli Wang et al. (2021) from MOSEL, we successfully gathered sufficient training material for these languages and generated corresponding X→En translation pairs leveraging Granary pipeline.

English naturally dominates the dataset, comprising approximately 285,000 hours (40%) of ASR data. Given English's central role across all three tasks (ASR, X→En, En→X), this dominance supports building a solid foundational knowledge base during pretraining.

Figure 5 presents the training hours distribution for our 24 non-English target languages, revealing important patterns in data availability across tasks. Language imbalance mitigation strategies, including approaches to address English dominance, are detailed in Sections 3.3.1 and 4.3.

As observed in the Figure 5, the En→X translation direction exhibits relatively uniform data distribution across languages, with values consistently ranging between 20,000-29,000 hours. The primary divergence emerges in ASR and X→En translation tasks, where low-resource languages such as Ukrainian (790 hours), Maltese, Estonian, and Slovak contrast sharply with high-resource languages including Spanish, French, German, Italian, Portuguese, and Russian, which dominate with significantly higher training hours. Given this pronounced imbalance and the fact that VoxPopuli data from the Granary corpus serves as the primary ASR source, we further analyze the ASR data source composition in the subsequent Figure 6.

When examining the relative volumes of Granary sub-corpora and NeMo ASR Set 3.0 in the ASR data for each language under study, a clear trend emerges. Except for high-resource, well-represented languages such as German, Spanish, French, Italian, Portuguese, and Russian, the Voxpopuli subset of the Granary corpus dominates, comprising over 95% of the data for most languages. This dominance of Voxpopuli creates two primary issues for these languages: (a) Voxpopuli recordings originate from

[4] https://github.com/NVIDIA/NeMo-speech-data-processor/tree/main/dataset_configs/multilingual/granary

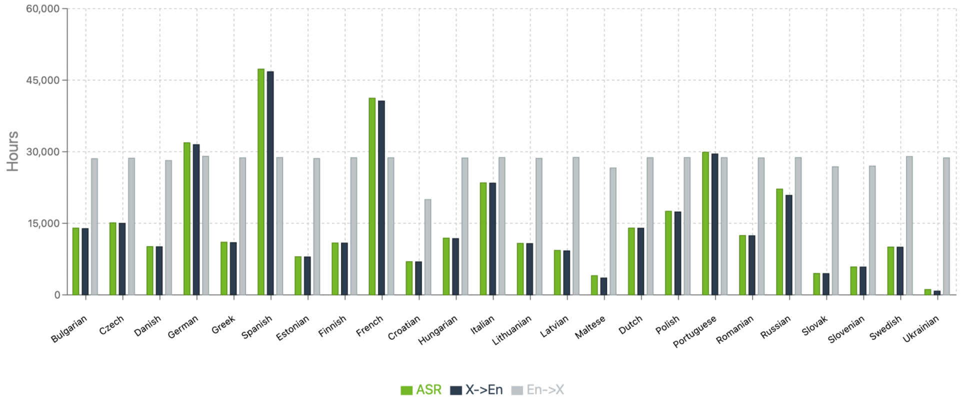

Figure 5: Language (non-English) Training Hours Distribution by Task.

EU parliament sessions, where the language register differs significantly from everyday conversational speech, leading to narrow-domain data dominance; and (b) Voxpopuli consists primarily of 30-second audio segments, which limits the acoustic and linguistic diversity available for languages dominated by this corpus. We reserve Voxpopuli audio resegmentation for future work. Despite these limitations, we cannot eliminate Voxpopuli entirely, as doing so would remove 15 unique languages from our 25-language set, contradicting our objective of supporting low-resource language inclusion.

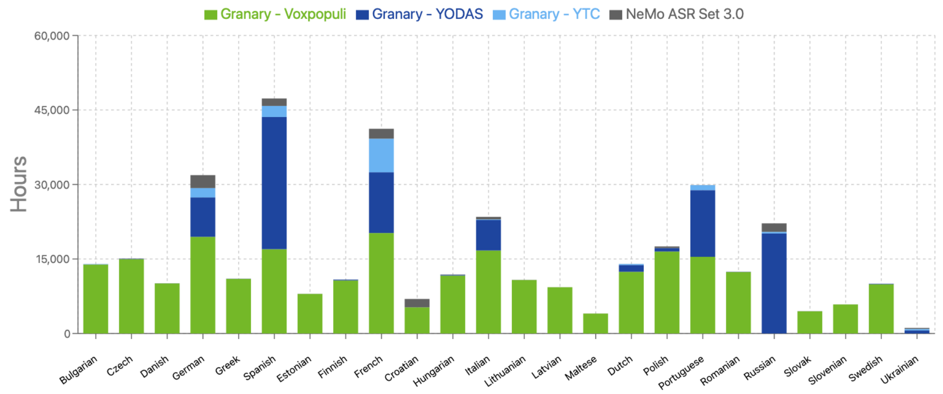

Figure 6: Language (non-English) ASR Data Training Hours Distribution by Corpus.

For detailed numerical breakdowns of training hours by language, corpus, and task, refer to Appendix A.

3.3.1 Balancing Languages and Corpora

Building on the preceding analysis of language and corpora imbalance, we adopt a two-tier sampling policy that (i) balances corpora *within* each language and (ii) balances *across* languages. During pre-training, each direction is treated as a distinct "language" entry (e.g., `lv`, `lv-en`, `en-lv`), so the policy applies uniformly to ASR and AST.

We followed the general methodology described in Babu et al. (2021), with one key modification. In Babu et al. (2021), the procedure first upsamples languages within a corpus and then balances the different corpora by treating each corpus as a separate language. In contrast, our approach inverts this order: we first perform corpus balancing within each language, and only then apply language balancing across the training corpora. This adjustment ensures that low-resource corpora within a language are not overshadowed before cross-language balancing is applied. Our procedure consists of three steps:

1. **Corpus balancing within language.** For a given language l, we first compute unnormalized weights for each corpus $c \in l$:
$$w_c = \left(\frac{n(c)}{N_l} \right)^{\alpha},$$
where $n(c)$ is the number of hours in corpus c, $N_l = \sum_{c \in l} n(c)$ is the total number of training hours for language l, and $\alpha \in (0, 1]$ is a subsampling factor controlling the trade-off between high-resource and low-resource corpora. The normalized distribution over corpora within language l is then
$$p_c = \frac{w_c}{\sum_{c \in l} w_c}, \quad \sum_{c \in l} p_c = 1.$$
2. **Language balancing across training corpora.** Next, we compute unnormalized weights for languages:
$$w_l = \left(\frac{n(l)}{N_{\text{total}}} \right)^{\beta},$$
where $n(l) = \sum_{c \in l} n(c)$ is the total number of hours for language l, $N_{\text{total}} = \sum_l n(l)$ is the global total across all languages, and $\beta \in (0, 1]$ is an upsampling factor controlling the degree of balance between high- and low-resource languages. The normalized distribution over languages is then
$$p_l = \frac{w_l}{\sum_{l'} w_{l'}}, \quad \sum_{l} p_l = 1.$$
3. **Final entry distribution.** The final probability of sampling from a corpus c in language l is the product
$$p_{c,l} = p_l \cdot p_c.$$

In practice, we set both the corpus-level subsampling factor and the language-level upsampling factor to $\alpha = 0.5$ and $\beta = 0.5$, respectively. Having computed these distributions, we leveraged the Lhotse multi-functional library Żelasko et al. (2021) to form batches according to $p_{c,l}$. This ensured diverse sampling at each step. Our analysis showed that, despite the inherent imbalance across languages and tasks, the upsampling procedure consistently produced batches containing at least 14 distinct language pairs.

3.4 Evaluation Benchmarks

Having established our training data composition, we now describe the evaluation benchmarks used to assess model performance across tasks and languages.

As canary-1b-v2 is multi-task model, it required comprehensive multi-task evaluation sets for assessment. For this purpose, we primarily used the FLEURS dataset, which included all 25 languages of our focus. In addition to the FLEURS dataset, we also utilized CoVoSTWang et al. (2020) and Multilingual LibriSpeech (MLS) data. The latter two datasets did not represent all 25 languages, but rather covered a subset of them. See Table 1 for complete details on the evaluation datasets and their language coverage.

In addition to these multilingual benchmarks, we evaluated our model on the Hugging Face Open ASR Leaderboard datasetsSrivastav et al. (2023) for comprehensive English ASR assessment and competitive benchmarking against other state-of-the-art models.

4 Training

The development of state-of-the-art multi-task and multi-language models necessitates a training paradigm that goes beyond traditional methods. Modern large-scale training is typically a two-stage process that separates the acquisition of broad, general knowledge from the refinement of task-specific skills.

	ASR			**X→En**		**En→X**	
Lang	Fleurs	MLS	CoVoST2	Fleurs	CoVoST2	Fleurs	CoVoST2
bg	✓	–	–	✓	–	✓	–
cs	✓	–	–	✓	–	✓	–
da	✓	–	–	✓	–	✓	–
de	✓	–	✓	✓	✓	✓	✓
el	✓	–	–	✓	–	✓	–
en	✓	–	✓	–	–	–	–
es	✓	✓	✓	✓	✓	✓	–
et	✓	–	✓	✓	✓	✓	✓
fi	✓	–	–	✓	–	✓	–
fr	✓	✓	✓	✓	✓	✓	–
hr	✓	–	–	✓	–	✓	–
hu	✓	–	–	✓	–	✓	–
it	✓	✓	✓	✓	✓	✓	–
lt	✓	–	–	✓	–	✓	–
lv	✓	–	✓	✓	✓	✓	✓
mt	✓	–	–	✓	–	✓	–
nl	✓	✓	✓	✓	✓	✓	–
pl	✓	✓	–	✓	–	✓	–
pt	✓	✓	✓	✓	✓	✓	–
ro	✓	–	–	✓	–	✓	–
ru	✓	–	✓	✓	✓	✓	–
sk	✓	–	–	✓	–	✓	–
sl	✓	–	✓	✓	✓	✓	✓
sv	✓	–	✓	✓	✓	✓	✓
uk	✓	–	✓	✓	–	✓	–

Table 1: Language coverage by task and dataset in evaluation set. A checkmark indicates that language is present in the corresponding dataset for the given task.

The first phase, pre-training, is foundational: the model is exposed to vast amounts of unlabeled or weakly supervised data. The goal is to capture fundamental statistical patterns of language and speech, thereby establishing a robust general foundation. Without this stage, training each new task from scratch would demand prohibitively large labeled datasets and computational resources.

The second phase, fine-tuning, adapts this general foundation to specific tasks or domains using smaller, task-oriented labeled datasets. This stage allows for targeted improvements, making the model more effective in practical scenarios. In our work, we employ this two-stage paradigm as well, leveraging fine-tuning as a mitigation strategy for data-related challenges.

A crucial component underpinning both stages is the tokenizer, which determines how raw text or speech transcriptions are decomposed into units that the model can process. The quality and design of the tokenizer directly affect training efficiency and downstream performance, especially in multilingual and multi-task contexts Abagyan et al. (2025). Because of this central role, tokenizer training merits dedicated discussion, which we provide in the next subsection.

4.1 Tokenizer Training

Unlike the initial versions of the Canary model, which employed concatenated tokenizers Dhawan et al. (2023), we trained a unified tokenizer for all 25 included languages in this work. This decision was motivated by three key factors. First, preliminary experiments comparing unified and concatenated tokenizers in identical setups demonstrated that the unified tokenizer significantly outperformed the concatenated approach. Second, a unified tokenizer enables natural code-switching functionality, which is essential given that Granary data, the primary source for Canary-1B-v2 training, contains multilingual content where words from different languages appear within single-language datasets.

Third, a unified tokenizer provides a consistent lexical space that serves as a strong foundation for downstream techniques such as phrase and word boosting.

To ensure balanced representation across all 25 languages and avoid under-representation of low-resource languages, we trained the SentencePiece tokenizer Kudo & Richardson (2018) on a carefully constructed dataset. The core of this training set was our En→X portion of the training data, which, as shown in Figure 5, is uniformly balanced across non-English languages. To complement this, we added English text from the YouTube subset (YTC, YODAS) of the Granary corpus as well as from NeMo ASR Set 3.0. This diverse domain selection was intended to prevent tokenizer vocabulary from overfitting to narrow-domain datasets (e.g., VoxPopuli parliamentary language).

We conducted experiments with three vocabulary sizes: 4,096, 8,192, and 16,384 tokens. These vocabularies include 1,162 special tokens specific to Canary model prompts, encompassing task-defining tokens such as <|*timestamps*|>, <|*notimestamps*|>, language ID tokens, and other placeholder special tokens. Our experiments consistently showed that larger vocabulary sizes yielded better downstream performance on both ASR and AST tasks. Furthermore, unified tokenizers with sizes 8,192 and 16,384 demonstrated similar compression rates, indicating an optimal balance between downstream performance and compression efficiency. Table 2 illustrates compression rate comparisons on the FLEURS dataset, comparing two different Canary tokenizer sizes against GPT-4oOpenAI et al. (2024) tokenizer compression rates as baseline. Notably, our tokenizers achieve both improved average compression rates and substantially lower standard deviations, suggesting more consistent behavior across languages. This stability can be attributed to balancing the amount of text per language in the overall corpus supplied to SentencePiece tokenizer training, which effectively mitigates drastic cross-lingual variations in compression rates.

	GPT-4o	Canary-1B-v2 (vocab 8,192)	Canary-1B-v2 (vocab 16,384)
Mean (μ)	3.513	2.534	2.849
Std. Dev. (σ)	0.662	0.220	0.230

Table 2: Compression rate comparisons on the FLEURS dataset across all 25 languages, comparing two Canary tokenizer sizes against GPT-4o as the baseline.

Based on these analyses, Canary-1B-v2 employs a unified BPE tokenizerSennrich et al. (2016) to handle input across all 25 languages, providing robust multilingual processing capabilities while maintaining computational efficiency.

4.2 Pre-training

To mimic the human learning process, which has long been observed as a multi-stage progression, we designed our pre-training to follow a two-stage process. In the first stage, the Canary model was trained on X→En (360,000 hours), English ASR (285,000 hours), and non-speech data (1,200 hours) for 150,000 steps on 64 NVIDIA A100 GPUs. The best configuration used a learning rate of 4e-4 with a minimum of 1e-6, 5,000 warm-up steps, and an inverse square-root learning rate scheduleVaswani et al. (2023). The AdamW optimizerLoshchilov & Hutter (2019) with weight decay of 0.001 was applied. Training was initialized from a FastConformer Hybrid RNN-T/CTC checkpoint that had been trained on four languages (English, Spanish, German, and French) for ASR task. The training data was divided into duration bins using NeMo's implementation of 2D duration bucket estimation[5], which was then combined with Lhotse dynamic bucketing. To maximize GPU usage, OOMptimizerŻelasko et al. (2024) was employed to determine the maximum feasible batch size for each bucket, and GPU utilization remained consistently high at around 95% throughout this stage.

After completing the first stage, training continued from the resulting checkpoint on the full blend of data (ASR, X→En, and En→X), comprising roughly 1.7 million hours, for an additional 100,000 steps. A more detailed breakdown of the task composition is provided in Section 3.1. We observed performance saturation when training was extended beyond this point. The best results were obtained with a learning rate of 3e-4 and 5,000 warm-up steps, while other settings remained unchanged from the first stage.

[5] https://github.com/NVIDIA-NeMo/NeMo/blob/main/scripts/speech_recognition/estimate_duration_bins_2d.py

Regime	**Model**	HF Leaderboard (En)	FLEURS (25)	MLS (5)	CoVoST2 (13)
Two-stage	X→En	7.54%	-	-	-
	X→En + ASR + En→X	8.36%	11.03%	**7.21%**	8.31%
Single-stage	X→En + ASR + En→X	**7.73%**	**10.66%**	7.35%	**8.11%**

(a) ASR results (WER). Lower is better.

Regime	**Model**	FLEURS (24)	CoVoST2 (11)
Two-stage	X→En	70.57	77.25
	X→En + ASR + En→X	**73.23**	**75.76**
Single-stage	X→En + ASR + En→X	73.18	75.39

(b) AST (X→En) results (COMET). Higher is better.

Regime	**Model**	FLEURS (24)	CoVoST2 (5)
Two-stage	X→En + ASR + En→X	83.86	80.14
Single-stage	X→En + ASR + En→X	**84.30**	**80.63**

(c) AST (En→X) results (COMET). Higher is better.

Table 3: Comparison of Two-stage vs. Single-stage models across ASR and AST benchmarks.
[*] COMET scores computed with `Unbabel/wmt22-comet-da`.

In parallel, we trained a single-stage baseline model. Starting from the same FastConformer Hybrid RNN-T/CTC checkpoint, this model was trained on the full dataset from the outset for 250,000 steps, using the same optimization setup described above.

Table 3 compares the two approaches. The results are close overall, with each approach slightly outperforming the other in certain cases. However, across evaluations we consistently observed that X→En scores fell short of SOTA results, and the two-stage model performed slightly better in this direction. For this reason, we selected the two-stage checkpoint for subsequent fine-tuning. An additional advantage of the two-stage setup lies in its efficiency for experimentation. In the single-stage regime, every trial with the full dataset requires training for the entire 250,000 steps, since the model must simultaneously learn both the foundational representations and the interactions between tasks. By contrast, in the two-stage regime the first stage already establishes a strong foundation. As a result, the second stage needs only around 100,000 additional steps on the full dataset to adapt and integrate task mixtures. This makes it possible to freely vary weighting schemes or data compositions in the second stage for experimentation purposes without incurring the cost of retraining the model for 250,000 steps each time.

Parakeet-TDT-0.6B-v3 was initialized from a multilingual CTC checkpoint pre-trained on the Granary ASR subset and trained for 150,000 steps on 128 A100 GPUs with temperature-based sampling ($\alpha = 0.5$ and $\beta = 0.5$) to balance corpora and languages, as described in Section 3.3.1.

4.3 Fine-tuning

As discussed in Section 3.3, a recurring challenge in our training pipeline is single-corpus or domain domination, which affects more than half of the supported languages. This has already impacted our results: for instance, we consistently observed unusually low (below SOTA) performance in the X→En direction, where VoxPopuli dominance is particularly evident.

To mitigate this and other imbalances in the pre-training data, we extended the pre-trained checkpoint with a a third high-quality fine-tuning stage. Importantly, this fine-tuning does not introduce a new task or domain but instead focuses the model on a high-quality subset of the training data. This subset includes NeMo ASR Set 3.0 and the YouTube portion of the Granary dataset for ASR and X→En, as well as our supplementary dataset for En→X. Additionally, we filtered the translation training data by QE scores[6]Gowda et al. (2023), keeping only samples with QE > 0.85. Thus, beyond mitigating corpus dominance, this stage also addresses quality imbalances within individual corpora.

To further balance tasks and languages, we constructed the training data as follows: for each language pair, we selected 200 hours of data from the high-quality subset. If fewer than 200 hours were available, the remainder was filled with other data (including VoxPopuli when necessary). This construction strategy was based on similar steps followed for *parakeet-tdt-0.6b-v2*[7] , where it had already yielded remarkable results. The complete training set was then divided into four equally weighted groups: ASR (non-English) (4,800 h), X→En (4,800 h), En→X (4,800 h), and English ASR (600 h). During training, sampling was balanced across groups, with each group selected with equal probability. Within each group, language pairs were also equally likely to be sampled, since their data volumes were normalized to 200 hours per pair.

With this configuration, we fine-tuned for 10k additional steps (without warm-up) using inverse square-root scheduling. The best performance was achieved with a learning rate of 2e-5 and a minimum of 1e-6.

In addition, we explored an alternative setup inspired by Parmar et al. (2024), where high-quality subsets are introduced at points in training when the learning rate is most suitable to absorb a shift in data distribution. We extended this approach by manipulating sampling weights dynamically during training. Specifically, at each dataloader step, language and corpus weights were gradually adjusted from an initial imbalance toward the target balance. This avoids "shocking" the model at the beginning of fine-tuning and instead enables a smoother adaptation. In our case, we again used the four-group configuration, balancing languages and corpora within each group as described in Section 3.3.1 ($\alpha = 0.2, \beta = 0.5$). Over the 10,000 fine-tuning steps, weights transitioned from the start values to the target uniform distribution (1 / number of languages in a group) according to a cosine schedule. We also experimented with linear and exponential schedules, but cosine yielded the most stable and robust results. An example of this setup is shown in Figure 7, where as fine-tuning progresses and the learning rate decreases, the MOSEL dataset weight gradually decreases, while the FLEURS dataset weight which is considered a high-quality dataset increases according to the predefined scheduler.

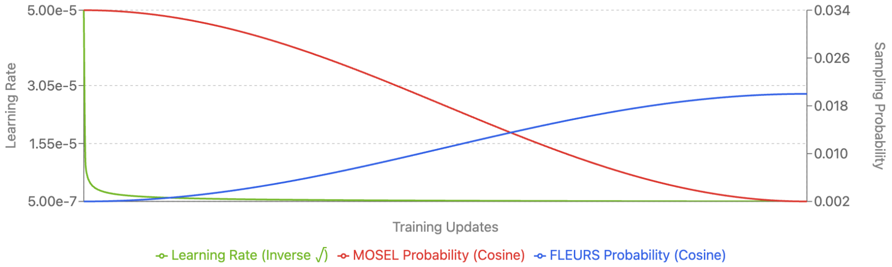

Figure 7: Example of Data Balancing Schedule. Green line shows the learning rate (inverse square root schedule), while red and blue lines represent MOSEL and FLEURS sampling probabilities (cosine schedules) along the fine-tuning process.

Table 4 presents the results of these two setups compared to the initial pre-trained checkpoint. Fine-tuning with rebalanced data distribution successfully mitigated narrow-domain and corpus imbalance effects for ASR and X→En tasks. Improvements are particularly visible on the FLEURS dataset, which offers cleaner and more controlled evaluation conditions than CoVoST2. We achieved an 6 absolute COMET improvement (73.23 → 79.30) for X→En, and a 25% relative WER reduction (11.03% → 8.40%) for ASR. As expected, En→X performance remained stable across setups, since the original pre-training distribution for this direction was already well-balanced.

Comparing the two fine-tuning strategies, overall performance is similar, with the exception of ASR on CoVoST2, where weight scheduling yielded a 1.5% absolute WER gain. Since CoVoST2 is the most spontaneous of our benchmarks, we hypothesize that weight scheduling prevents "catastrophic

[6] QE scores computed with `Unbabel/wmt22-comet-da`

[7] `https://huggingface.co/nvidia/parakeet-tdt-0.6b-v2`

Model	HF Leaderboard (En)	FLEURS (25)	MLS (5)	CoVoST2 (13)
Pre-trained baseline	8.36%	11.03%	7.21%	8.31%
Fine-tuned (15k HQ)	**7.15%**	8.69%	**7.11%**	10.33%
Fine-tuned (Balancing schedule)	**7.15%**	**8.40%**	7.27%	**8.85%**

(a) ASR results (WER). Lower is better.

Model	FLEURS (24)	CoVoST2 (11)
Pre-trained baseline	73.23	75.76
Fine-tuned (15k HQ)	79.27	76.82
Fine-tuned (Balancing schedule)	**79.30**	**77.48**

(b) AST (X→En) results (COMET). Higher is better.

Model	FLEURS (24)	CoVoST2 (5)
Pre-trained baseline	83.86	80.14
Fine-tuned (15k HQ)	84.38	**80.32**
Fine-tuned (Balancing schedule)	**84.56**	80.29

(c) AST (En→X) results (COMET). Higher is better.

Table 4: Comparison of pre-trained vs. fine-tuned models across ASR and AST benchmarks.

forgetting” of pre-trained knowledge, whereas fine-tuning only on 15k hours of clean data biases the model too strongly toward clearer speech. Moreover, weight scheduling consistently extracted more performance from the available data, leading to additional gains in the X→En direction.

In light of these findings, we release the weight-scheduled fine-tuned model as our primary version and continue to explore data balancing schedules to better understand their benefits and broader applicability.

Fine-tuning stage for *Parakeet-TDT-0.6B-v3* ran for 5,000 steps on 4 A100 GPUs using 7,500 hours of high-quality NeMo ASR Set 3.0 data.

5 Timestamps

5.1 Timestamps Generation in Attention-Encoder Decoder Models

The extraction of precise timestamps from spoken words is a critical capability of modern Speech Recognition systems, essential for powering downstream applications such as timed subtitling and content retrieval. The methods for extracting timestamps from attention-based speech recognition models are diverse, ranging from post-processing techniques to architectural redesigns. Each approach represents a different trade-off between accuracy, computational overhead, and architectural complexity.

The architecture that we are working with in Canary-1B-v2 is an attention-based encoder-decoder (AED) system. In these models, alignment between audio frames and text tokens is handled during the decoding phase. This is primarily facilitated by the cross-attention mechanism, which produces a weight matrix representing the probabilistic correlation between each output token and every input audio frame. While these weights provide a "soft" alignment, they are prone to non-monotonicity, where the attention path can jump back and forth in time, leading to a certain degree of inherent unreliability or "fuzziness."

5.1.1 Post-Processing with Dynamic Time Warping (DTW)

To convert this soft, often non-monotonic alignment into precise, word-level boundaries, a robust post-processing algorithm like Dynamic Time Warping (DTW)Giorgino (2009) is applied to the cross-attention matrix. DTW finds the optimal, non-linear alignment path between two sequences by computing a cumulative cost or score matrix. In this context, it aligns the sequence of output tokens with the sequence of input audio frames by finding the path of highest cumulative attention scores. This process effectively "hardens" the fuzzy attention into a clear, monotonic sequence of word boundaries, providing the start and end times for each word. A prominent example of this method is its use in third-party implementationsLouradour (2023) for WhisperRadford et al. (2023) model, which natively provides only segment-level timestamps.

5.1.2 Predictive Timestamp Generation

A fundamentally different approach is to embed timestamp prediction directly into the AED model itself. In this setup, timestamping is reframed as a core predictive task rather than a post-processing step. Whisper Radford et al. (2023) first introduced this strategy by training on a corpus in which special frame-number tokens (e.g., <|*0*|>*,* <|*1*|>*,* . . .) were inserted into transcriptions at segment boundaries. The Canary model Hu et al. (2025) subsequently adopted and extended this approach by inserting the tokens at word boundaries. By learning to predict these tokens directly, the model incorporates an understanding of acoustic–temporal relationships into its core predictive capability.

This approach has distinct advantages, as it shifts the alignment burden to the model's training process. However, it also introduces new complexities:

- **Data Curation:** The creation of a diverse and well-represented training corpus with accurate timestamp tokens requires significant computational resources and careful data curation.
- **Training Challenges:** The model must now learn an additional task, which can create balancing issues and requires a more carefully tuned training regimen to avoid negatively impacting transcription accuracy.

5.1.3 Forced Alignment as a Standalone Method

For many production and commercial applicationsBain et al. (2023), the process of timestamping has been abstracted away into a service. Forced alignment, a method that takes an audio file and its corresponding transcript to generate timestamps, serves as a powerful standalone. Given the complexities and potential instability of relying solely on "soft" attention weights or multi-task learning for timestamps, we explored exactly the forced alignment method as a standalone approach for Canary-1B-v2. Unlike the methods above, it does not rely on the end-to-end model's internal alignment mechanism for timestamping.

For our purposes, the NeMo Forced Aligner (NFA)Rastorgueva et al. (2023) has proven to be an effective method for generating word and segment-level timestamps in Hu et al. (2025). This method has become the backbone for timestamp extraction in our system, used in conjunction with auxiliary Multilingual Parakeet CTC model.

5.2 NeMo Forced Aligner (NFA)

NeMo Forced Aligner (NFA) is a tool for generating token-, word-, and segment-level timestamps of speech in audio using CTC-based ASR models. Optionally, NFA can align ground truth text with the CTC-based ASR model decoder's log-probabilities. The alignment process uses Viterbi decoding to find the most probable alignment of given tokens based on log-probabilities from the CTC head.

Figure 8a depicts the timestamp generation process for Canary-1B-v2 speech recognition output using NFA capabilities. This pipeline incorporates an additional ASR model, a Parakeet architecture model with CTC decoder comprising 600M parameters. This model was trained using the same unified tokenizer as Canary-1B-v2 for 250,000 steps on 128 NVIDIA A100 GPUs, using the ASR subset of Canary-1B-v2 training data described in Section 3. When integrating the Forced Alignment pipeline into Canary-1B-v2's inference pipeline, a critical question emerged regarding ASR and AST task alignment: Can NFA effectively align translated speech with audio sequences in completely different languages?

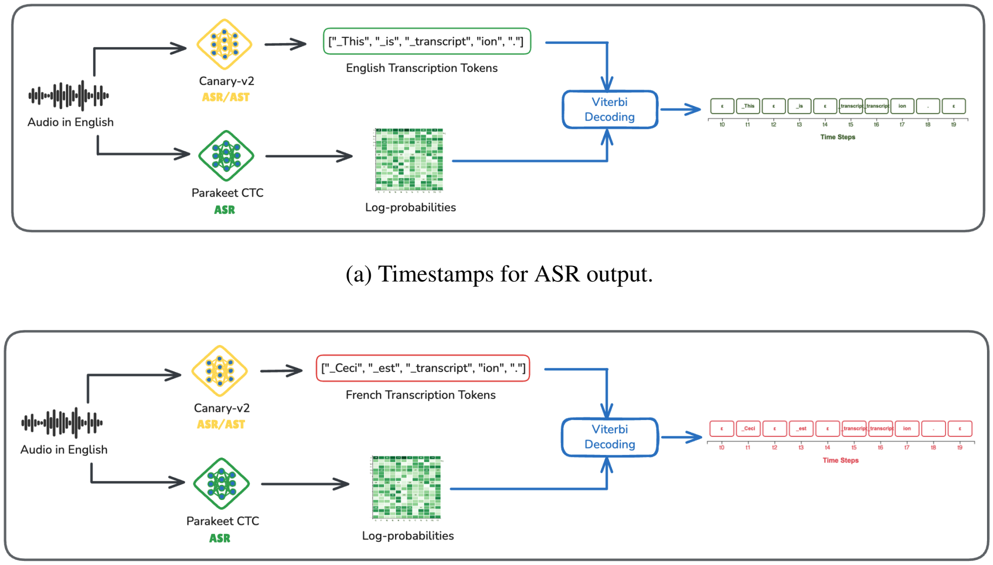

(a) Timestamps for ASR output.

(b) Timestamps for AST output.

Figure 8: Overview of Timestamps Generation for Canary-1B-v2 with NFA.

ASR alignment is typically monotonic, maintaining a strictly sequential, left-to-right mapping from temporal audio frames to output phonemes, characters, or words. This "forced alignment" ensures linear correspondence between transcription output and input speech signal. In contrast, AST alignment is both non-monotonic and cross-lingual. Words and phrases in the source language lack direct, sequential correspondence with translated target language output due to linguistic phenomena including different grammatical structures, verb tenses, and word orders. For example, the English phrase *I love you* translates to French *je t'aime*, where source and target word orders don't align sequentially.

Additionally, the CTC model (Parakeet CTC) incorporated into the NFA pipeline is trained solely for ASR tasks and lacks AST knowledge.

To evaluate timestamp generation capabilities for AST tasks, we conducted experiments on evaluation benchmarks and performed manual evaluation of the generated timestamps. The NFA pipeline integrated into Canary-1B-v2's inference mechanism successfully produced high-quality segment-level timestamps, as shown in Figure 8b. We therefore recommend using segment-level timestamps with translation outputs, as word-level timestamps can be inaccurate due to the non-monotonic nature of speech translation. An example of segment-level timestamps with the respective prompts is illustrated in Figure 9.

Overall, we observed that the current pipeline with NFA yields consistently reliable timestamping performance. We attribute this in part to the fact that our evaluation scope primarily covers European languages, where translations to and from English tend to preserve sentence structure without drastic reordering. By contrast, languages with more divergent syntactic structures such as Mandarin may introduce substantial shifts in word and phrase order. As such, while the results within our explored language set are promising, the applicability of the NFA pipeline to typologically distant languages remains uncertain and warrants more thorough testing and investigation.

Looking ahead, future work will focus on more comprehensive and quantitative AST timestamp evaluation and on exploring how log-probabilities of an ASR model are effectively leveraged for aligning translation transcript tokens.

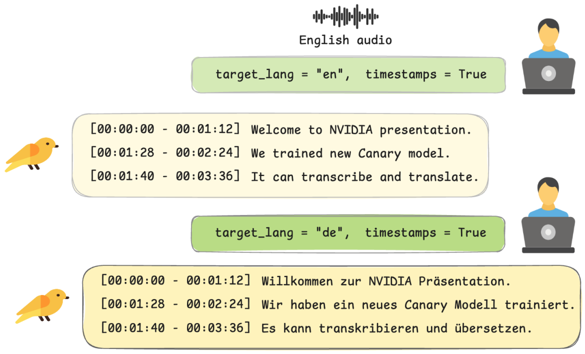

```
target_lang = "en",  timestamps = True
```

```
[00:00:00 - 00:01:12] Welcome to NVIDIA presentation.
[00:01:28 - 00:02:24] We trained new Canary model.
[00:01:40 - 00:03:36] It can transcribe and translate.
```

```
target_lang = "de",  timestamps = True
```

```
[00:00:00 - 00:01:12] Willkommen zur NVIDIA Präsentation.
[00:01:28 - 00:02:24] Wir haben ein neues Canary Modell trainiert.
[00:01:40 - 00:03:36] Es kann transkribieren und übersetzen.
```

Figure 9: Examples of Canary-1B-v2 output along with segment-level timestamps.

6 Evaluation

The evaluation of the final *Canary-1B-v2* model is conducted using the benchmark suites introduced in Section 3.4. For comparative analysis, we consider several strong baselines: *Whisper-large-v3* (1.55B), *seamless-m4t-v2-large* (2.3B), and *seamless-m4t-medium* (1.2B), as they are the closest in scale to *Canary-1B-v2* among seamless speech models. In addition, we include *Voxtral-Mini-3B-2507*Liu et al. (2025) (3B) and *Phi-4-multimodal-instruct*Abouelenin et al. (2025) (5.6B), two multimodal and LLM-based systems, in order to highlight the trade-offs between accuracy and inference efficiency where *Canary-1B-v2* provides an advantage. Our second release, *Parakeet-TDT-0.6B-v3*, is likewise included in the multilingual ASR evaluations.

Multilingual evaluations in this section are reported under two complementary settings:

1. **All supported languages:** 24 total, excluding Latvian, which is not supported by *seamless-m4t-v2-large* or *seamless-m4t-medium*.
2. **Common languages:** 6 shared by all compared models (*en*, *fr*, *de*, *it*, *pt*, and *es*).

6.1 ASR Performance

For ASR performance evaluation, we report normalized WER (%). We use the Hugging Face Open Automatic Speech Recognition Leaderboard normalizers[8]: the English normalizer for English test sets, and the newly added multilingual normalizer for non-English test sets. Both remove punctuation and lowercase the text. The English normalizer further performs richer, language-specific normalization (e.g., numbers, abbreviations, currencies), whereas the multilingual normalizer emphasizes cross-language consistency by replacing symbols and punctuation-like markers with spaces and by mapping or stripping diacritics to their base forms.

6.1.1 English ASR (HuggingFace Leaderboard) Performance

Table 5 presents the results for the Hugging Face Leaderboard datasets, calculated with the official repository and reported on the Hugging Face Open ASR Leaderboard. Notably, *Canary-1B-v2* outperforms *Whisper-large-v3* on the official average WER metric, while also achieving remarkable inference efficiency. With an RTFx of 749, *Canary-1B-v2* runs approximately 7–10 times faster than the other evaluated models, highlighting its strength in balancing accuracy with throughput efficiency.

Additionally, *Parakeet-TDT-0.6B-v3* attains the highest throughput among all systems (RTFx $=$ 3332.74) while maintaining a low average WER of 6.32%, within 0.18 absolute points of *Phi-4-multimodal-instruct* (6.14%). This corresponds to $\approx 54\times$ faster inference than *Phi-4-multimodal-instruct*, combining near–state-of-the-art accuracy with extreme throughput.

[8] https://github.com/huggingface/open_asr_leaderboard/tree/main/normalizer

Model	RTFx	Avg WER	AMI	Earnings22	Gigaspeech	LS Clean	LS Other	SPGI	TED-LIUM	VoxPopuli
Whisper-large-v3	145.51	7.44	15.95	11.29	10.02	2.01	3.91	2.94	3.86	9.54
Voxtral-Mini-3B-2507	109.86	7.05	16.31	10.65	10.24	1.89	4.08	2.37	3.70	7.14
Phi-4-multimodal-instruct	62.12	6.14	11.45	10.50	9.77	1.67	3.82	3.11	2.89	5.93
Parakeet-TDT-0.6B-v3	3332.74	6.32	11.39	11.19	9.57	1.92	3.59	3.98	2.8	6.09
Canary-1B-v2	749.00	7.15	16.01	11.79	10.82	2.18	3.56	2.28	4.29	6.25

Table 5: ASR performance (WER %) and inference efficiency (RTFx) on Hugging Face OpenASR Leaderboard benchmarks.

6.1.2 Multilingual ASR Performance

As is seen in Figure 10, *Canary-1B-v2* demonstrates consistently strong multilingual ASR performance across both the full 24-language set and the common 6-language subset. On the full evaluation, computed as an average across three different datasets (FLEURS, CoVoST, MLS), it achieves an average WER of around 8.1%, outperforming *whisper-large-v3* (9.9%) and *seamless-m4t-medium* (12.0%), while remaining only slightly behind the much larger and heavier *seamless-m4t-v2-large* (7.2%). On the common-language evaluation, also averaged across the same three datasets, *Canary-1B-v2* reaches 5.2% WER compared to 5.8% for *whisper-large-v3* and 8.2% for *seamless-m4t-medium*, and in fact slightly outperforms *seamless-m4t-v2-large* (5.3%). Even though other models are specialized in this smaller set, *Canary-1B-v2* supports 19 additional languages while still matching or surpassing much heavier and LLM-powered baselines.

Additionally, the companion 0.6B model *Parakeet-TDT-0.6B-v3* averages 9.7% WER across the 24-language evaluation (11.52/9.78/7.83 on FLEURS/CoVoST/MLS), edging past *whisper-large-v3* (9.9%) while trailing *Canary-1B-v2* (8.1%) and *seamless-m4t-v2-large* (7.2%). On the common-language subset it reaches 5.3% WER (4.37/4.79/6.74), essentially matching *seamless-m4t-v2-large* (5.3%) and outperforming *whisper-large-v3* (5.8%).

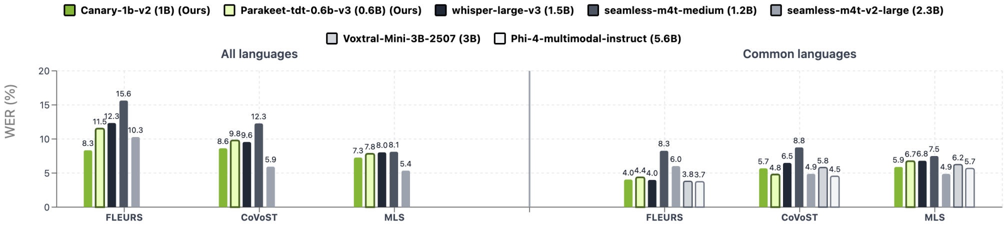

Figure 10: Multilingual ASR performance of *Canary-1B-v2* and *Parakeet-TDT-0.6B-v3* compared to baseline models on both 24-language and 6-language subsets.

Per-language WERs for each evaluation benchmark are provided in the Appendix B

6.1.3 Noise-robustness evaluation

Table 6 reports the robustness of *Canary-1B-v2* and *Parakeet-TDT-0.6B-v3* across different Signal-to-Noise Ratios (SNR) on the LibriSpeech Clean test setPanayotov et al. (2015), where MUSAN music and noise samples Snyder et al. (2015) were added.

Interestingly, we observe that performance of *Canary-1B-v2* slightly improves when decreasing the SNR from 100 to 25, with WER dropping from 2.18% to 2.01%. This suggests that *Canary-1B-v2* benefits from a small amount of background noise, likely due to training on large-scale datasets that naturally include noisy conditions, such as the YouTube subset of the Granary corpus and VoxPopuli, where background noise from live interpreters and other sources is present. This indicates that the model has learned to leverage noisy input scenarios, resulting in improved robustness.

Complementing this, *Parakeet-TDT-0.6B-v3* is consistently more robust across SNRs (1.92–1.96% WER from 100 to 25 dB) and outperforming under severe noise with 12.21% at −5 dB vs 19.38% for *Canary-1B-v2* (∼37% relative).

Model	SNR (dB) 100	50	25	10	5	0	-5
Parakeet-TDT-0.6B-v3	**1.92**	**1.92**	1.96	2.15	2.62	4.82	12.21
Canary-1B-v2	2.18	2.16	**2.01**	2.29	2.80	5.08	19.38

Table 6: WER (%) across different SNR levels on the LibriSpeech Clean test set with MUSAN music and noise samples.

6.2 AST Performance

For AST performance we consider two evaluation directions: X→En En and En → X. We again used the evaluation benchmarks introduced in Section 3.4.

In terms of performance metrics, we report both COMET and BLEUPapineni et al. (2002) scores. COMET is used as the primary metric throughout this section, while BLEU scores are reported in Appendix C and D. BLEU, being based on n-gram overlap, often underestimates semantic adequacy when translations diverge lexically or syntactically from reference sentences but remain valid. This makes BLEU less reliable, especially in multilingual and low-resource settings. COMET, in contrast, leverages pretrained multilingual encoders and human-annotated data, enabling it to better capture semantic similarity and translation quality beyond surface-level word overlap. As such, COMET provides a more faithful reflection of translation performance, while BLEU is included for completeness and comparability with prior work.

6.2.1 X→En Performance

As shown in Figure 11, *Canary-1B-v2* outperforms *whisper-large-v3* and *seamless-m4t-medium* by a large margin across both evaluation benchmarks. On the full-language setting, it achieves 79.28 COMET on FLEURS and 78.14 on CoVoST2, compared to 76.51 / 74.61 for *whisper-large-v3* and 77.30 / 75.64 for *seamless-m4t-medium*. Even against the much larger *seamless-m4t-v2-large* (81.71 / 80.26), *Canary-1B-v2* remains close despite having less than half the parameters.

On the common-language evaluation, *Canary-1B-v2* continues to perform strongly, reaching 82.41 COMET on FLEURS and 79.07 on CoVoST. This is competitive with the heavier *seamless-m4t-v2-large* (82.84 / 80.16) and even the LLM-powered *Voxtral-Mini-3B-2507* (84.53 / 78.90) and *Phi-4-multimodal-instruct* (84.06 / 80.11). Notably, on the more spontaneous and noisy CoVoST2 dataset, *Canary-1B-v2* performs particularly well (79.07 vs. 76.86 for *whisper-large-v3*), increasing the gap over the *whisper* model, comparable to the *Phi-4-multimodal-instruct* (80.11), and even outperforming the *Voxtral-Mini-3B-2507* (78.90). This reflects the robustness learned from large-scale noisy training sources.

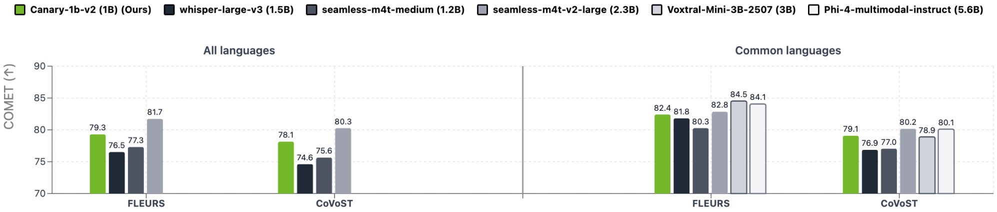

Figure 11: AST (X→En) performance of *Canary-1B-v2* compared to baseline models on both 24-language and 6-language subsets.

6.2.2 En→X Performance

As shown in Figure 12, *Canary-1B-v2* achieves strong En→X performance. On FLEURS, it remains on par with the much larger *seamless-m4t-v2-large* in the all-language setting (84.47 vs. 84.85

COMET) and even slightly outperforms all compared models in the supported-language evaluation (83.79 vs. 83.56 for *seamless-m4t-v2-large*, 82.20 for *Phi-4*, and 83.56 for *Voxtral-Mini-3B-2507*). On CoVoST2, however, *Canary-1B-v2* lags behind *seamless-m4t-v2-large* (80.03 vs. 82.66 in the all-language setting, and 78.37 vs. 81.30 in the supported-language evaluation). A possible explanation is that while the En→X training data covers diverse domains, the X-language ASR pathways were more strongly shaped by narrower-domain data, leading the decoder to generalize less effectively to spontaneous CoVoST speech.

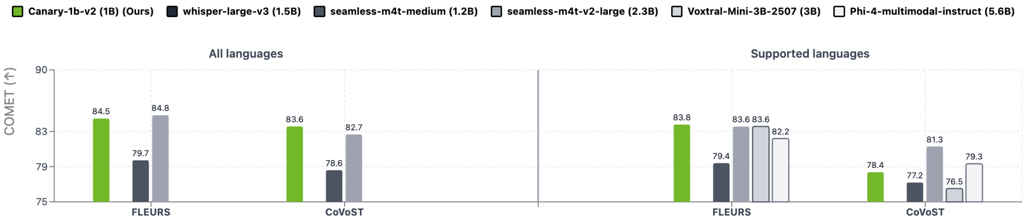

Figure 12: AST (En→X) performance of *Canary-1B-v2* compared to baseline models on both 24-language and 6-language subsets.

6.3 nGPT and FastConformer comparison

To better understand the capabilities of nGPT as an encoder, we trained models of different scales on the Granary datasets. These experiments were designed to assess how well nGPT scales and how it compares to the FastConformer baseline across ASR and AST benchmarks.

As shown in Table 7, scaling from 1B to 3B parameters consistently improved performance. The 3B-parameter nGPT model demonstrated stronger generalization across tasks, with especially notable gains on the challenging X→EN translation benchmark—where FastConformer struggled most. Importantly, the 3B model achieved these results within a single training stage and only 100k steps. While the 1B model falls short of the 3B across tasks, it still shows the same generalization trend and remains competitive, particularly on translation.

In contrast, FastConformer required a more elaborate multi-stage training regime to achieve strong results. With sufficient fine-tuning, however, it was able to surpass nGPT in all tasks. This highlights a key distinction: nGPT is a data-hungry model that thrives under large-scale training and quickly reaches competitive performance, whereas FastConformer benefits more from fine-tuning and exhibits greater relative improvements in low-data scenarios.

6.4 Longform inference

Neural encoders are typically trained on relatively short input sequences, which means they often fail to generalize well when faced with significantly longer contexts at inference time. For ASR, this limitation becomes especially clear when transcribing utterances beyond the average training length (e.g., >40 seconds). As context length grows, models exhibit degraded stability and accuracy, making it essential to explore strategies that overcome this bottleneck.

One class of solutions modifies the inference procedure rather than the model architecture itself. A common approach is local attention Rekesh et al. (2023b), where each query token attends only to a fixed-size window of neighboring tokens instead of the entire sequence. This sliding-window design reduces quadratic attention costs and stabilizes inference on long inputs, while still capturing the local dependencies most critical for recognition tasks. In practice, such methods can be readily applied in models with CTC or RNN-T heads, making them an effective strategy for scaling ASR systems to longer contexts. The other method is chunking mechanism in which audio is divided into smaller segments that are transcribed separately and then merged and it can easily be adapted to encoder–decoder architectures.

Model	**Regime**	HF Leaderboard (En)	FLEURS (25)	MLS (5)	CoVoST2 (13)
FC 1B	1st stage	7.73%	10.66%	7.35%	8.11%
nGPT 1B	1st stage	8.94%	9.94%	8.11%	9.96%
nGPT 3B	1st stage	7.73%	10.18%	8.35%	10.48%
FC 1B	3-stage (15k HQ)	7.15%	8.69%	7.11%	10.33%
nGPT 3B	2-stage (15k HQ)	7.32%	10.31%	8.32%	10.30%

(a) ASR results (WER). Lower is better.

Model	**Regime**	FLEURS (24)	CoVoST2 (11)
FC 1B	1st stage	73.18	75.39
nGPT 1B	1st stage	76.72	74.02
nGPT 3B	1st stage	78.36	75.75
FC 1B	3-stage (15k HQ)	79.27	76.82
nGPT 3B	2-stage (15k HQ)	79.14	75.90

(b) AST (X→En) results (COMET). Higher is better.

Model	**Regime**	FLEURS (24)	CoVoST2 (5)
FC 1B	1st stage	84.30	80.63
nGPT 1B	1st stage	83.05	78.31
nGPT 3B	1st stage	84.22	80.00
FC 1B	3-stage (15k HQ)	84.38	80.32
nGPT 3B	2-stage (15k HQ)	84.28	79.48

(c) AST (En→X) results (COMET). Higher is better.

Table 7: Comparison of FC and nGPT across training regimes on ASR and AST benchmarks.
* COMET scores computed with `Unbabel/wmt22-comet-da`.

6.4.1 Chunk based approach

For our current FastConformer encoder paired with a Transformer decoder, we employed a dynamic parallel chunking mechanism to enable efficient long-form inference. Each input audio file is segmented into chunks of 30–40 seconds, where the exact length is chosen dynamically to minimize padding in the final chunk. To preserve continuity across boundaries, adjacent chunks overlap by 1 second.

The chunked segments are then fed into the model in parallel as separate entries within a batch. After the model produces transcriptions for all segments, the outputs are merged into a single hypothesis. To resolve overlapping regions, we apply a Longest Common Subsequence (LCS) algorithm at the token level, ensuring that duplicated text in the overlap regions is removed from the final transcript.

For very long recordings (longer than one hour), we further segment the audio into hour-long blocks, each processed independently using the same chunking and merging procedure. This hierarchical design ensures scalability to arbitrarily long audio while maintaining both efficiency and transcription quality.

We compared this method with chunking inference without overlap, where fixed audio chunks were processed sequentially through the model one by one, and observed clear performance gains. Table 8 summarizes the results. Parallel chunking achieves lower WER and significantly higher RTFx on both benchmarks compared to script-based sequential chunking. On the Earnings22 dataset, WER improved from 15.61% to 13.93%, while RTFx increased almost 4×. Similarly, on the TAL(10h) dataset, WER dropped from 16.62% to 10.12%, and RTFx more than doubled.

Table 8: Comparison of two chunking mechanisms for long-form inference. In parallel chunking(ours), audio is split into overlapping chunks that are processed simultaneously within a batch, with overlaps later merged to maintain continuity. In *sequential chunking*, fixed-length chunks are processed one by one without overlap, and outputs are concatenated directly.

	ASR Earnings22		**ASR TAL (10h)**	
Method	EN (%)	RTFx	EN (%)	RTFx
Parallel Chunking (Ours)	**13.93**	**144.244**	**10.12**	**64.067**
Sequential Chunking (30 sec)	15.61	37.17	16.62	26.88

6.4.2 POSTIONAL ENCODINGS FOR LONGFORM INFERENCE

While inference-time strategies such as local attention and chunking mitigate some of the difficulties of long-context transcription, they do not fully address the underlying limitations of how models represent positional information. To complement these approaches, we explored alternative positional encodings within the nGPT-based encoder, focusing on Rotary Position Embeddings (RoPE) and Attention with Linear Biases (ALiBi), and further adapting them to better suit long-form ASR.

13 shows Word Error Rate (WER) on the Earnings dataset across different evaluation lengths (20, 40, 60, 80, and 100 seconds). We observe that in the baseline implementations, ALiBi consistently outperforms RoPE for longer sequences, although both exhibit increasing WER as the context length grows.

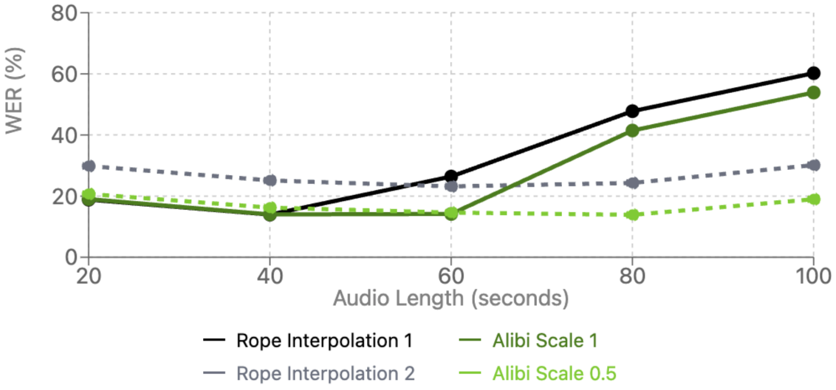

Figure 13: Comparison of Attention with Linear Biases (ALiBi) and Rotary Position Embeddings (RoPE) on long-form ASR with the Earnings dataset. For RoPE, larger interpolation factors correspond to reducing the angular rotation step to better accommodate longer sequences. For ALiBi, smaller scaling factors apply a lighter penalty to distant tokens, allowing the model to attend further into the context.

To improve generalization for nGPT encoder architecture, we modified each positional encoding. For RoPE, we reduced the angular rotation applied at each position so that longer input sequences would span the same effective angular spectrum as those seen during training. For ALiBi, we adjusted the bias scaling factor, which controls how strongly distant tokens are down-weighted, thereby allowing the model to retain more attention to faraway context. These adjustments significantly reduced WER across all lengths. Nevertheless, ALiBi remained more effective than RoPE in long-context ASR, highlighting the benefit of incorporating distance-aware attention biases in encoder-style speech tasks.

Empirically, the two approaches demonstrated task-dependent behavior. In ASR, ALiBi showed improvements, likely because reducing emphasis on distant tokens is not detrimental for speech recognition, where local context dominates. In contrast, for AST, long-range context is more critical, and we found RoPE to be more effective. These results highlight that positional encoding strategies interact differently with downstream tasks: ALiBi favors efficiency in short-to-mid context alignment, whereas RoPE better supports tasks requiring global context retention.

7 Conclusions

This report introduces ***Canary-1B-v2*** and ***Parakeet-TDT-0.6B-v3***, two multilingual models that achieve state-of-the-art ASR and AST performance with high efficiency. The models were developed through a comprehensive exploration of data, training strategies, and architecture. This included curating a 1.7M-hour dataset with non-speech audio to reduce hallucinations and using dynamic weight scheduling to mitigate data imbalance.

A core contribution of this work is a comparative study of encoder architectures, featuring the first application of nGPT to speech processing. Our experiments reveal a crucial trade-off: while the final FastConformer-based model excelled after a multi-stage training and fine-tuning regimen , the nGPT encoder is a data-hungry model that demonstrated stronger and faster generalization in large-scale, single-stage training, especially on challenging translation tasks. This investigation also yielded novel insights into positional encodings, finding ALiBi more effective for long-form ASR and RoPE more suitable for AST.

We also present a robust method for generating accurate segment-level timestamps using the NeMo Forced Aligner , and the release of Parakeet-TDT-0.6B-v3 extends high-quality ASR to resource-limited settings.

References

Diana Abagyan, Alejandro R. Salamanca, Andres Felipe Cruz-Salinas, Kris Cao, Hangyu Lin, Acyr Locatelli, Marzieh Fadaee, Ahmet Üstün, and Sara Hooker. One tokenizer to rule them all: Emergent language plasticity via multilingual tokenizers, 2025. URL https://arxiv.org/abs/2506.10766.

Ahmed Abouelenin et al. Phi-4-Multimodal: Compact yet Powerful Multimodal Foundation Model. *arXiv preprint arXiv:2503.01743*, 2025.

R. Ardila, M. Branson, K. Davis, M. Henretty, M. Kohler, J. Meyer, R. Morais, L. Saunders, F. M. Tyers, and G. Weber. Common voice: A massively-multilingual speech corpus. In *Proceedings of the 12th Conference on Language Resources and Evaluation (LREC 2020)*, pp. 4211–4215, 2020.

Arun Babu, Changhan Wang, Andros Tjandra, Kushal Lakhotia, Qiantong Xu, Naman Goyal, Kritika Singh, Patrick von Platen, Yatharth Saraf, Juan Pino, Alexei Baevski, Alexis Conneau, and Michael Auli. Xls-r: Self-supervised cross-lingual speech representation learning at scale, 2021. URL https://arxiv.org/abs/2111.09296.

Max Bain, Jaesung Huh, Tengda Han, and Andrew Zisserman. Whisperx: Time-accurate speech transcription of long-form audio, 2023. URL https://arxiv.org/abs/2303.00747.

Laurent Barrault and Others. SeamlessM4T: Massively Multilingual & Multimodal Machine Translation. *arXiv preprint arXiv:2308.11596*, 2023.

Zhehuai Chen, He Huang, Andrei Andrusenko, et al. SALM: Speech-Augmented Language Model with In-Context Learning for Speech Recognition and Translation. *arXiv preprint arXiv:2310.09424*, 2023.

Zhehuai Chen, He Huang, Andrei Andrusenko, Oleksii Hrinchuk, Krishna C Puvvada, Jason Li, Subhankar Ghosh, Jagadeesh Balam, and Boris Ginsburg. Salm: Speech-augmented language model with in-context learning for speech recognition and translation. In *ICASSP 2024-2024 IEEE International Conference on Acoustics, Speech and Signal Processing (ICASSP)*, pp. 13521–13525. IEEE, 2024a.

Zhehuai Chen, He Huang, Oleksii Hrinchuk, Krishna C Puvvada, Nithin Rao Koluguri, Piotr Żelasko, Jagadeesh Balam, and Boris Ginsburg. Bestow: Efficient and streamable speech language model with the best of two worlds in gpt and t5. In *2024 IEEE Spoken Language Technology Workshop (SLT)*, pp. 147–154. IEEE, 2024b.

Alexis Conneau, Min Ma, Simran Khanuja, Yu Zhang, Vera Axelrod, Siddharth Dalmia, Jason Riesa, Clara Rivera, and Ankur Bapna. Fleurs: Few-shot learning evaluation of universal representations of speech, 2022. URL https://arxiv.org/abs/2205.12446.

Kunal Dhawan, Dima Rekesh, and Boris Ginsburg. Unified model for code-switching speech recognition and language identification based on a concatenated tokenizer, 2023. URL https://arxiv.org/abs/2306.08753.

Linhao Dong, Shuang Xu, and Bo Xu. Speech-transformer: a no-recurrence sequence-to-sequence model for speech recognition. In *2018 IEEE international conference on acoustics, speech and signal processing (ICASSP)*, pp. 5884–5888. IEEE, 2018.

Marco Gaido, Sara Papi, Luisa Bentivogli, Alessio Brutti, Mauro Cettolo, Roberto Gretter, Marco Matassoni, Mohamed Nabih, and Matteo Negri. Mosel: 950,000 hours of speech data for open-source speech foundation model training on eu languages. *arXiv preprint arXiv:2410.01036*, 2024.

Toni Giorgino. Computing and visualizing dynamic time warping alignments in r: The dtw package. *Journal of Statistical Software*, 31(7):1–24, 2009. doi: 10.18637/jss.v031.i07. URL https://www.jstatsoft.org/index.php/jss/article/view/v031i07.

Thamme Gowda, Tom Kocmi, and Marcin Junczys-Dowmunt. Cometoid: Distilling strong reference-based machine translation metrics into Even stronger quality estimation metrics. In Philipp Koehn, Barry Haddon, Tom Kocmi, and Christof Monz (eds.), *Proceedings of the Eighth Conference on Machine Translation*, pp. 751–755, Singapore, December 2023. Association for Computational Linguistics. URL https://aclanthology.org/2023.wmt-1.62.

Alex Graves, Santiago Fernández, Faustino Gomez, and Jürgen Schmidhuber. Connectionist temporal classification: labelling unsegmented sequence data with recurrent neural networks. In *Proceedings of the 23rd international conference on Machine learning*, pp. 369–376, 2006.

Anmol Gulati and Others. Conformer: Convolution-augmented Transformer for Speech Recognition. In *Interspeech*, 2020.

Ke Hu, Krishna Puvvada, Elena Rastorgueva, Zhehuai Chen, He Huang, Shuoyang Ding, Kunal Dhawan, Hainan Xu, Jagadeesh Balam, and Boris Ginsburg. Word level timestamp generation for automatic speech recognition and translation, 2025. URL https://arxiv.org/abs/2505.15646.

Mayank Jain et al. RNN-T for Latency Controlled ASR with Improved Beam Search. *arXiv preprint arXiv:1911.01629*, 2019.

Nikolay Karpov, Alexander Denisenko, and Fedor Minkin. Golos: Russian dataset for speech research, 2021. URL https://arxiv.org/abs/2106.10161.

Nithin Rao Koluguri, Monica Sekoyan, George Zelenfroynd, Sasha Meister, Shuoyang Ding, Sofia Kostandian, He Huang, Nikolay Karpov, Jagadeesh Balam, Vitaly Lavrukhin, Yifan Peng, Sara Papi, Marco Gaido, Alessio Brutti, and Boris Ginsburg. Granary: Speech recognition and translation dataset in 25 european languages, 2025. URL https://arxiv.org/abs/2505.13404.

Wessel Kraaij, Thomas Hain, Mike Lincoln, and Wilfried Post. The ami meeting corpus. In *Proc. International Conference on Methods and Techniques in Behavioral Research*, pp. 1–4, 2005.

Taku Kudo and John Richardson. Sentencepiece: A simple and language independent subword tokenizer and detokenizer for neural text processing, 2018. URL https://arxiv.org/abs/1808.06226.

Xinjian Li, Shinnosuke Takamichi, Takaaki Saeki, William Chen, Sayaka Shiota, and Shinji Watanabe. Yodas: Youtube-oriented dataset for audio and speech, 2024. URL https://arxiv.org/abs/2406.00899.

Alexander H. Liu, Andy Ehrenberg, Andy Lo, Clément Denoix, Corentin Barreau, Guillaume Lample, Jean-Malo Delignon, Khyathi Raghavi Chandu, Patrick von Platen, Pavankumar Reddy Muddireddy, Sanchit Gandhi, Soham Ghosh, Srijan Mishra, Thomas Foubert, Abhinav Rastogi, Adam Yang, Albert Q. Jiang, Alexandre Sablayrolles, Amélie Héliou, Amélie Martin, Anmol Agarwal, Antoine Roux, Arthur Darcet, Arthur Mensch, Baptiste Bout, Baptiste Rozière, Baudouin De Monicault, Chris Bamford, Christian Wallenwein, Christophe Renaudin, Clémence

Lanfranchi, Darius Dabert, Devendra Singh Chaplot, Devon Mizelle, Diego de las Casas, Elliot Chane-Sane, Emilien Fugier, Emma Bou Hanna, Gabrielle Berrada, Gauthier Delerce, Gauthier Guinet, Georgii Novikov, Guillaume Martin, Himanshu Jaju, Jan Ludziejewski, Jason Rute, Jean-Hadrien Chabran, Jessica Chudnovsky, Joachim Studnia, Joep Barmentlo, Jonas Amar, Josselin Somerville Roberts, Julien Denize, Karan Saxena, Karmesh Yadav, Kartik Khandelwal, Kush Jain, Lélio Renard Lavaud, Léonard Blier, Lingxiao Zhao, Louis Martin, Lucile Saulnier, Luyu Gao, Marie Pellat, Mathilde Guillaumin, Mathis Felardos, Matthieu Dinot, Maxime Darrin, Maximilian Augustin, Mickaël Seznec, Neha Gupta, Nikhil Raghuraman, Olivier Duchenne, Patricia Wang, Patryk Saffer, Paul Jacob, Paul Wambergue, Paula Kurylowicz, Philomène Chagniot, Pierre Stock, Pravesh Agrawal, Rémi Delacourt, Romain Sauvestre, Roman Soletskyi, Sagar Vaze, Sandeep Subramanian, Saurabh Garg, Shashwat Dalal, Siddharth Gandhi, Sumukh Aithal, Szymon Antoniak, Teven Le Scao, Thibault Schueller, Thibaut Lavril, Thomas Robert, Thomas Wang, Timothée Lacroix, Tom Bewley, Valeriia Nemychnikova, Victor Paltz, Virgile Richard, Wen-Ding Li, William Marshall, Xuanyu Zhang, Yihan Wan, and Yunhao Tang. Voxtral, 2025. URL https://arxiv.org/abs/2507.13264.

Ilya Loshchilov and Frank Hutter. Decoupled weight decay regularization, 2019. URL https://arxiv.org/abs/1711.05101.

Ilya Loshchilov, Cheng-Ping Hsieh, Simeng Sun, and Boris Ginsburg. ngpt: Normalized transformer with representation learning on the hypersphere. *arXiv preprint arXiv:2410.01131*, 2024.

Jérôme Louradour. whisper-timestamped. https://github.com/linto-ai/whisper-timestamped, 2023.

OpenAI, :, Aaron Hurst, Adam Lerer, Adam P. Goucher, Adam Perelman, Aditya Ramesh, Aidan Clark, AJ Ostrow, Akila Welihinda, Alan Hayes, Alec Radford, Aleksander Mądry, Alex Baker-Whitcomb, Alex Beutel, Alex Borzunov, Alex Carney, Alex Chow, Alex Kirillov, Alex Nichol, Alex Paino, Alex Renzin, Alex Tachard Passos, Alexander Kirillov, Alexi Christakis, Alexis Conneau, Ali Kamali, Allan Jabri, Allison Moyer, Allison Tam, Amadou Crookes, Amin Tootoochian, Amin Tootoonchian, Ananya Kumar, Andrea Vallone, Andrej Karpathy, Andrew Braunstein, Andrew Cann, Andrew Codispoti, Andrew Galu, Andrew Kondrich, Andrew Tulloch, Andrey Mishchenko, Angela Baek, Angela Jiang, Antoine Pelisse, Antonia Woodford, Anuj Gosalia, Arka Dhar, Ashley Pantuliano, Avi Nayak, Avital Oliver, Barret Zoph, Behrooz Ghorbani, Ben Leimberger, Ben Rossen, Ben Sokolowsky, Ben Wang, Benjamin Zweig, Beth Hoover, Blake Samic, Bob McGrew, Bobby Spero, Bogo Giertler, Bowen Cheng, Brad Lightcap, Brandon Walkin, Brendan Quinn, Brian Guarraci, Brian Hsu, Bright Kellogg, Brydon Eastman, Camillo Lugaresi, Carroll Wainwright, Cary Bassin, Cary Hudson, Casey Chu, Chad Nelson, Chak Li, Chan Jun Shern, Channing Conger, Charlotte Barette, Chelsea Voss, Chen Ding, Cheng Lu, Chong Zhang, Chris Beaumont, Chris Hallacy, Chris Koch, Christian Gibson, Christina Kim, Christine Choi, Christine McLeavey, Christopher Hesse, Claudia Fischer, Clemens Winter, Coley Czarnecki, Colin Jarvis, Colin Wei, Constantin Koumouzelis, Dane Sherburn, Daniel Kappler, Daniel Levin, Daniel Levy, David Carr, David Farhi, David Mely, David Robinson, David Sasaki, Denny Jin, Dev Valladares, Dimitris Tsipras, Doug Li, Duc Phong Nguyen, Duncan Findlay, Edede Oiwoh, Edmund Wong, Ehsan Asdar, Elizabeth Proehl, Elizabeth Yang, Eric Antonow, Eric Kramer, Eric Peterson, Eric Sigler, Eric Wallace, Eugene Brevdo, Evan Mays, Farzad Khorasani, Felipe Petroski Such, Filippo Raso, Francis Zhang, Fred von Lohmann, Freddie Sulit, Gabriel Goh, Gene Oden, Geoff Salmon, Giulio Starace, Greg Brockman, Hadi Salman, Haiming Bao, Haitang Hu, Hannah Wong, Haoyu Wang, Heather Schmidt, Heather Whitney, Heewoo Jun, Hendrik Kirchner, Henrique Ponde de Oliveira Pinto, Hongyu Ren, Huiwen Chang, Hyung Won Chung, Ian Kivlichan, Ian O'Connell, Ian O'Connell, Ian Osband, Ian Silber, Ian Sohl, Ibrahim Okuyucu, Ikai Lan, Ilya Kostrikov, Ilya Sutskever, Ingmar Kanitscheider, Ishaan Gulrajani, Jacob Coxon, Jacob Menick, Jakub Pachocki, James Aung, James Betker, James Crooks, James Lennon, Jamie Kiros, Jan Leike, Jane Park, Jason Kwon, Jason Phang, Jason Teplitz, Jason Wei, Jason Wolfe, Jay Chen, Jeff Harris, Jenia Varavva, Jessica Gan Lee, Jessica Shieh, Ji Lin, Jiahui Yu, Jiayi Weng, Jie Tang, Jieqi Yu, Joanne Jang, Joaquin Quinonero Candela, Joe Beutler, Joe Landers, Joel Parish, Johannes Heidecke, John Schulman, Jonathan Lachman, Jonathan McKay, Jonathan Uesato, Jonathan Ward, Jong Wook Kim, Joost Huizinga, Jordan Sitkin, Jos Kraaijeveld, Josh Gross, Josh Kaplan, Josh Snyder, Joshua Achiam, Joy Jiao, Joyce Lee, Juntang Zhuang, Justyn Harriman, Kai Fricke, Kai Hayashi, Karan Singhal, Katy Shi, Kavin Karthik, Kayla Wood, Kendra

Rimbach, Kenny Hsu, Kenny Nguyen, Keren Gu-Lemberg, Kevin Button, Kevin Liu, Kiel Howe, Krithika Muthukumar, Kyle Luther, Lama Ahmad, Larry Kai, Lauren Itow, Lauren Workman, Leher Pathak, Leo Chen, Li Jing, Lia Guy, Liam Fedus, Liang Zhou, Lien Mamitsuka, Lilian Weng, Lindsay McCallum, Lindsey Held, Long Ouyang, Louis Feuvrier, Lu Zhang, Lukas Kondraciuk, Lukasz Kaiser, Luke Hewitt, Luke Metz, Lyric Doshi, Mada Aflak, Maddie Simens, Madelaine Boyd, Madeleine Thompson, Marat Dukhan, Mark Chen, Mark Gray, Mark Hudnall, Marvin Zhang, Marwan Aljubeh, Mateusz Litwin, Matthew Zeng, Max Johnson, Maya Shetty, Mayank Gupta, Meghan Shah, Mehmet Yatbaz, Meng Jia Yang, Mengchao Zhong, Mia Glaese, Mianna Chen, Michael Janner, Michael Lampe, Michael Petrov, Michael Wu, Michele Wang, Michelle Fradin, Michelle Pokrass, Miguel Castro, Miguel Oom Temudo de Castro, Mikhail Pavlov, Miles Brundage, Miles Wang, Minal Khan, Mira Murati, Mo Bavarian, Molly Lin, Murat Yesildal, Nacho Soto, Natalia Gimelshein, Natalie Cone, Natalie Staudacher, Natalie Summers, Natan LaFontaine, Neil Chowdhury, Nick Ryder, Nick Stathas, Nick Turley, Nik Tezak, Niko Felix, Nithanth Kudige, Nitish Keskar, Noah Deutsch, Noel Bundick, Nora Puckett, Ofir Nachum, Ola Okelola, Oleg Boiko, Oleg Murk, Oliver Jaffe, Olivia Watkins, Olivier Godement, Owen Campbell-Moore, Patrick Chao, Paul McMillan, Pavel Belov, Peng Su, Peter Bak, Peter Bakkum, Peter Deng, Peter Dolan, Peter Hoeschele, Peter Welinder, Phil Tillet, Philip Pronin, Philippe Tillet, Prafulla Dhariwal, Qiming Yuan, Rachel Dias, Rachel Lim, Rahul Arora, Rajan Troll, Randall Lin, Rapha Gontijo Lopes, Raul Puri, Reah Miyara, Reimar Leike, Renaud Gaubert, Reza Zamani, Ricky Wang, Rob Donnelly, Rob Honsby, Rocky Smith, Rohan Sahai, Rohit Ramchandani, Romain Huet, Rory Carmichael, Rowan Zellers, Roy Chen, Ruby Chen, Ruslan Nigmatullin, Ryan Cheu, Saachi Jain, Sam Altman, Sam Schoenholz, Sam Toizer, Samuel Miserendino, Sandhini Agarwal, Sara Culver, Scott Ethersmith, Scott Gray, Sean Grove, Sean Metzger, Shamez Hermani, Shantanu Jain, Shengjia Zhao, Sherwin Wu, Shino Jomoto, Shirong Wu, Shuaiqi, Xia, Sonia Phene, Spencer Papay, Srinivas Narayanan, Steve Coffey, Steve Lee, Stewart Hall, Suchir Balaji, Tal Broda, Tal Stramer, Tao Xu, Tarun Gogineni, Taya Christianson, Ted Sanders, Tejal Patwardhan, Thomas Cunninghman, Thomas Degry, Thomas Dimson, Thomas Raoux, Thomas Shadwell, Tianhao Zheng, Todd Underwood, Todor Markov, Toki Sherbakov, Tom Rubin, Tom Stasi, Tomer Kaftan, Tristan Heywood, Troy Peterson, Tyce Walters, Tyna Eloundou, Valerie Qi, Veit Moeller, Vinnie Monaco, Vishal Kuo, Vlad Fomenko, Wayne Chang, Weiyi Zheng, Wenda Zhou, Wesam Manassra, Will Sheu, Wojciech Zaremba, Yash Patil, Yilei Qian, Yongjik Kim, Youlong Cheng, Yu Zhang, Yuchen He, Yuchen Zhang, Yujia Jin, Yunxing Dai, and Yury Malkov. Gpt-4o system card, 2024. URL `https://arxiv.org/abs/2410.21276`.

Vassil Panayotov, Guoguo Chen, Daniel Povey, and Sanjeev Khudanpur. Librispeech: An asr corpus based on public domain audio books. In *2015 IEEE International Conference on Acoustics, Speech and Signal Processing (ICASSP)*, pp. 5206–5210, 2015. doi: 10.1109/ICASSP.2015.7178964.

Kishore Papineni, Salim Roukos, Todd Ward, and Wei-Jing Zhu. Bleu: a method for automatic evaluation of machine translation. In *Proceedings of the 40th annual meeting of the Association for Computational Linguistics*, pp. 311–318, 2002.

Jupinder Parmar, Sanjev Satheesh, Mostofa Patwary, Mohammad Shoeybi, and Bryan Catanzaro. Reuse, don't retrain: A recipe for continued pretraining of language models, 2024. URL `https://arxiv.org/abs/2407.07263`.

Pleias. Youtube-commons: A massive open corpus for conversational and multimodal data, 2025. URL `https://huggingface.co/blog/Pclanglais/youtube-commons`. Dataset.

Vineel Pratap, Qiantong Xu, Anuroop Sriram, Gabriel Synnaeve, and Ronan Collobert. Mls: A large-scale multilingual dataset for speech research. *ArXiv*, abs/2012.03411, 2020.

Ofir Press, Noah A. Smith, and Mike Lewis. Train short, test long: Attention with linear biases enables input length extrapolation. In *International Conference on Learning Representations (ICLR)*, 2022.

Alec Radford, Jong Wook Kim, Tao Xu, Greg Brockman, Christine McLeavey, and Ilya Sutskever. Robust Speech Recognition via Large-Scale Weak Supervision. In *International Conference on Machine Learning (ICML)*, 2023.

Elena Rastorgueva, Vitaly Lavrukhin, and Boris Ginsburg. Nemo forced aligner and its application to word alignment for subtitle generation. In *Interspeech 2023*, pp. 5257–5258, 2023.

Dima Rekesh, Nithin Rao Koluguri, Samuel Kriman, and et al. FastConformer with Linearly Scalable Attention for Efficient Speech Recognition. *arXiv preprint arXiv:2305.05084*, 2023a.

Dima Rekesh, Nithin Rao Koluguri, Samuel Kriman, Somshubra Majumdar, Vahid Noroozi, He Huang, Oleksii Hrinchuk, Krishna Puvvada, Ankur Kumar, Jagadeesh Balam, et al. Fast conformer with linearly scalable attention for efficient speech recognition. In *2023 IEEE Automatic Speech Recognition and Understanding Workshop (ASRU)*, pp. 1–8. IEEE, 2023b.

Rico Sennrich, Barry Haddow, and Alexandra Birch. Neural machine translation of rare words with subword units. In Katrin Erk and Noah A. Smith (eds.), *Proceedings of the 54th Annual Meeting of the Association for Computational Linguistics (Volume 1: Long Papers)*, pp. 1715–1725, Berlin, Germany, August 2016. Association for Computational Linguistics. doi: 10.18653/v1/P16-1162. URL https://aclanthology.org/P16-1162/.

David Snyder, Guoguo Chen, and Daniel Povey. Musan: A music, speech, and noise corpus, 2015. URL https://arxiv.org/abs/1510.08484.

Vaibhav Srivastav, Somshubra Majumdar, Nithin Koluguri, Adel Moumen, Sanchit Gandhi, Hugging Face Team, Nvidia NeMo Team, and SpeechBrain Team. Open automatic speech recognition leaderboard.
urlhttps://huggingface.co/spaces/huggingface.co/spaces/open-asr-leaderboard/leaderboard, 2023.

Jianlin Su, Yu Lu, Shengfeng Pan, Ahmed Murtadha, Bo Wen, and Yunfeng Liu. Roformer: Enhanced transformer with rotary position embedding. In *Advances in Knowledge Discovery and Data Mining (PAKDD)*, 2021.

Ashish Vaswani, Noam Shazeer, Niki Parmar, Jakob Uszkoreit, Llion Jones, Aidan N. Gomez, Lukasz Kaiser, and Illia Polosukhin. Attention is all you need, 2023. URL https://arxiv.org/abs/1706.03762.

Changhan Wang, Anne Wu, and Juan Pino. Covost 2 and massively multilingual speech-to-text translation, 2020. URL https://arxiv.org/abs/2007.10310.

Changhan Wang, Morgane Rivière, Ann Lee, Anne Wu, Chaitanya Talnikar, Daniel Haziza, Mary Williamson, Juan Pino, and Emmanuel Dupoux. Voxpopuli: A large-scale multilingual speech corpus for representation learning, semi-supervised learning and interpretation, 2021. URL https://arxiv.org/abs/2101.00390.

Piotr Żelasko, Daniel Povey, Jan "Yenda" Trmal, and Sanjeev Khudanpur. Lhotse: a speech data representation library for the modern deep learning ecosystem, 2021. URL https://arxiv.org/abs/2110.12561.

Piotr Żelasko, Zhehuai Chen, Mengru Wang, Daniel Galvez, Oleksii Hrinchuk, Shuoyang Ding, Ke Hu, Jagadeesh Balam, Vitaly Lavrukhin, and Boris Ginsburg. Emmett: Efficient multimodal machine translation training, 2024. URL https://arxiv.org/abs/2409.13523.

Dong Zhang et al. SpeechGPT: Empowering Large Language Models with Intrinsic Cross-Modal Conversational Abilities. In *Findings of EMNLP*, 2023.

Appendix

Corpus	ASR	X→En	En→X	Total
Granary	638,229.73	358,284.40	-	996,514.13
NeMo ASR Set 3.0	19,843.10	10,165.01	197,020.66	227,028.77
Supplementary dataset	-	-	477,739.85	477,739.85
Total	658,072.83	368,449.41	674,760.51	1,701,282.75
Non-speech data				36,581.15
Grand Total				**1,737,863.91**

Table 9: Training data hours by corpus and tasks involved.

A Training Data Language, Corpora and Task Decomposition

Lang	ASR		X→En		En→X	
	Granary	NeMo	Granary	NeMo	NeMo	Supplementary
bg	13986.55	9.49	13875.61	9.30	8346.43	20194.40
cs	15043.85	58.56	14936.10	57.92	8408.30	20231.86
da	10104.41	13.08	10068.36	12.80	8041.09	20113.59
de	29279.61	2602.24	28974.96	2509.15	8781.31	20267.06
el	11008.78	24.89	10927.85	23.20	8472.81	20259.95
es	45812.67	1505.47	45353.29	1406.23	8505.52	20272.88
et	7983.65	10.54	7942.66	10.44	8453.49	20129.90
fi	10856.40	17.32	10841.47	17.00	8484.42	20262.53
fr	39226.50	1989.65	38626.92	1998.26	8482.86	20259.14
hr	5285.79	1671.12	5273.91	1646.91	5119.01	14850.72
hu	11818.71	65.15	11729.05	64.46	8452.52	20234.48
it	22962.30	515.16	22896.12	521.30	8515.96	20269.42
lt	10775.43	20.10	10731.04	19.70	8410.20	20213.40
lv	9311.46	8.58	9213.82	8.46	8663.14	20145.42
mt	4009.81	13.98	3524.11	13.67	7078.29	19519.90
nl	13997.41	9.64	13957.39	14.79	8477.62	20275.66
pl	17202.73	316.13	17071.60	308.58	8505.21	20272.97
pt	29869.11	16.99	29505.53	20.22	8478.27	20284.43
ro	12419.03	21.49	12368.69	21.20	8451.23	20253.89
ru	20460.39	1716.46	19595.31	1263.28	8511.02	20262.18
sk	4467.62	22.54	4439.20	21.67	7475.55	19374.72
sl	5851.59	9.41	5826.37	9.53	7688.19	19301.57
sv	10014.93	10.09	9991.90	9.88	8735.76	20253.51
uk	932.67	191.06	613.14	177.06	8482.46	20236.27
en	275548.32	9003.94	–	–	–	–

Table 10: Training data (hours) by language, corpora, and task. NeMo = NeMo ASR Set 3.0.

B Evaluation: ASR Performance

Model	**bg**	**cs**	**da**	**de**	**el**	**en**	**es**	**et**	**fi**	**fr**	**hr**	**hu**	**it**	**lt**	**lv**	**mt**	**nl**	**pl**	**pt**	**ro**	**ru**	**sk**	**sl**	**sv**	**uk**
whisper-large-v3	12.86	11.33	12.57	**4.30**	27.03	4.25	3.12	19.12	**7.70**	6.31	11.07	14.11	**2.31**	22.34	18.29	68.89	**5.57**	**4.74**	**3.65**	8.24	**4.17**	8.40	19.93	**7.88**	**6.51**
seamless-m4t-v2-large	10.67	9.31	12.09	6.25	25.68	6.15	5.10	**11.75**	12.24	6.82	11.89	**11.38**	4.49	15.47	–	**18.16**	8.15	8.76	7.32	8.87	7.43	7.42	**11.18**	11.13	9.07
seamless-m4t-medium	14.42	14.89	18.26	9.77	29.49	6.99	6.79	20.99	21.09	10.49	14.16	24.09	6.72	27.42	–	23.03	11.96	14.84	8.87	13.95	12.82	11.16	20.38	18.13	14.55
Voxtral-Mini-3B-2507	–	–	–	4.62	–	3.88	3.34	–	–	**4.63**	–	–	2.49	–	–	–	–	–	3.74	–	–	–	–	–	–
Phi-4-multimodal-instruct	–	–	–	4.37	–	**3.64**	3.23	–	–	4.64	–	–	2.48	–	–	–	–	–	4.00	–	–	–	–	–	–
Parakeet-TDT-0.6B-v3	12.64	11.01	18.41	5.04	20.70	4.85	3.45	17.73	13.21	5.15	12.46	15.72	3.00	20.35	22.84	20.46	7.48	7.31	4.76	12.44	5.51	8.82	24.03	15.08	6.79
Canary-1B-v2	**9.25**	**7.86**	**11.25**	4.40	**9.21**	4.50	**2.90**	12.55	8.59	5.02	**8.29**	12.90	3.07	**12.36**	**9.66**	18.31	6.12	6.64	4.39	**6.61**	6.90	**5.74**	13.32	9.57	10.50

Table 11: Per-language WER (%) results on the **FLEURS** benchmark.

Model	**es**	**fr**	**it**	**nl**	**pl**	**pt**
whisper-large-v3	4.89	7.15	9.26	12.08	8.88	5.96
seamless-m4t-v2-large	3.08	3.73	**6.83**	**6.91**	**5.74**	**5.86**
seamless-m4t-medium	4.43	6.08	10.13	8.57	10.22	9.36
Voxtral-Mini-3B-2507	3.85	5.75	9.36	–	–	5.87
Phi-4-multimodal-instruct	3.72	4.13	8.51	–	–	6.31
Parakeet-TDT-0.6B-v3	4.39	4.97	10.08	12.78	7.28	7.50
Canary-1B-v2	**2.94**	**3.36**	9.16	11.27	8.77	8.14

Table 12: Per-language WER (%) results on the **MLS** benchmark.

Model	**de**	**en**	**es**	**et**	**fr**	**it**	**lv**	**nl**	**pt**	**ru**	**sl**	**sv**	**uk**
whisper-large-v3	5.94	8.52	4.32	28.54	11.02	5.45	18.84	**5.97**	**3.72**	4.04	16.63	**8.06**	12.52
seamless-m4t-v2-large	5.34	**5.01**	4.20	**9.80**	6.44	4.46	–	**5.97**	3.87	**2.56**	**5.39**	9.20	9.01
seamless-m4t-medium	9.83	7.80	6.95	22.05	11.86	7.56	–	13.78	8.62	7.15	14.38	19.89	17.51
Voxtral-Mini-3B-2507	6.09	7.60	4.23	–	7.51	5.80	–	–	–	–	–	–	–
Phi-4-multimodal-instruct	**4.62**	5.83	3.81	–	6.61	**3.42**	–	–	–	–	–	–	–
Parakeet-TDT-0.6B-v3	4.84	6.80	**3.41**	22.04	**6.05**	3.69	38.36	6.50	3.96	3.00	31.80	20.16	**5.10**
Canary-1B-v2	5.53	6.85	3.81	18.28	6.30	4.80	**11.49**	6.93	6.87	5.14	7.59	13.32	18.15

Table 13: Per-language WER (%) results on the **CoVoST2** benchmark.

C Evaluation: AST (X→En) Performance

	bg		cs		da		de		el		es		et		fi		fr		hr		hu		it	
Model	C	B	C	B	C	B	C	B	C	B	C	B	C	B	C	B	C	B	C	B	C	B	C	B
whisper-large-v3	77.61	26.93	76.62	25.56	78.68	31.50	81.68	32.35	74.56	21.24	80.81	21.86	69.88	17.30	77.59	19.86	81.83	31.00	77.42	25.95	72.98	18.33	81.46	22.65
seamless-m4t-v2-large	**80.48**	**33.03**	**82.56**	**34.36**	**82.99**	**37.90**	83.98	37.38	**80.20**	**27.99**	81.94	25.56	**83.52**	**32.00**	**84.51**	**28.57**	82.77	33.77	**81.86**	**31.21**	**81.99**	**28.13**	82.92	26.76
seamless-m4t-medium	78.23	27.96	77.91	27.16	78.62	31.95	81.57	33.67	76.32	22.80	79.10	21.92	78.39	24.07	79.11	22.12	80.35	30.66	78.70	26.84	72.52	18.51	80.08	23.43
Voxtral-Mini-3B-2507	–	–	–	–	–	–	**85.01**	**38.47**	–	–	**83.73**	**28.32**	–	–	–	–	**84.33**	**35.84**	–	–	–	–	**84.19**	**29.31**
Phi-4-multimodal-instruct	–	–	–	–	–	–	84.93	38.16	–	–	82.85	25.66	–	–	–	–	83.88	35.28	–	–	–	–	83.62	26.44
Canary-1B-v2	79.60	30.93	78.64	29.28	80.45	34.80	83.09	36.03	76.73	24.08	81.19	25.45	80.25	28.38	80.81	24.68	82.80	34.10	78.48	29.09	76.86	24.26	82.03	25.57

	lt		lv		mt		nl		pl		pt		ro		ru		sk		sl		sv		uk	
Model	C	B	C	B	C	B	C	B	C	B	C	B	C	B	C	B	C	B	C	B	C	B	C	B
whisper-large-v3	65.05	13.69	66.11	15.40	54.96	12.18	79.57	22.12	77.43	20.90	83.22	37.63	81.07	30.34	80.72	26.56	76.70	23.35	70.12	17.27	81.07	34.28	78.71	27.95
seamless-m4t-v2-large	**77.98**	**24.53**	–	–	**74.02**	**41.18**	**82.23**	**28.01**	**79.98**	**24.85**	82.62	39.39	**83.21**	**35.26**	**81.85**	**30.27**	**82.13**	**33.03**	**80.52**	**26.62**	**83.13**	**38.05**	**81.86**	**33.34**
seamless-m4t-medium	69.29	17.00	–	–	70.43	34.68	79.00	23.07	74.33	18.73	80.18	34.72	78.83	29.58	78.29	24.03	78.94	27.07	72.79	19.45	77.61	30.71	77.20	25.76
Voxtral-Mini-3B-2507	–	–	–	–	–	–	–	–	–	–	**85.37**	43.00	–	–	–	–	–	–	–	–	–	–	–	–
Phi-4-multimodal-instruct	–	–	–	–	–	–	–	–	–	–	85.01	41.41	–	–	–	–	–	–	–	–	–	–	–	–
Canary-1B-v2	76.30	22.86	**79.71**	**27.86**	70.00	34.99	80.72	26.49	77.05	22.30	82.91	**39.43**	81.61	33.55	79.17	27.26	79.86	30.55	76.89	23.65	80.75	34.92	77.23	27.50

Table 14: Per-language COMET (C) and BLEU (B) scores (%) on the **FLEURS** benchmark.

	de		es		et		fr		it		lv		nl		pt		ru		sl		sv	
Model	C	B	C	B	C	B	C	B	C	B	C	B	C	B	C	B	C	B	C	B	C	B
whisper-large-v3	75.28	34.57	78.52	39.82	63.98	13.93	74.38	35.73	76.55	36.35	58.63	16.93	77.46	40.53	79.58	51.14	80.99	41.31	64.61	24.34	74.70	44.19
seamless-m4t-v2-large	**79.62**	**40.40**	**81.29**	43.47	**80.25**	**27.52**	**78.95**	**42.36**	80.05	40.49	–	–	**80.77**	**43.90**	80.89	**55.18**	**84.74**	**53.78**	**78.19**	**42.44**	**77.87**	**46.78**
seamless-m4t-medium	75.74	35.76	78.65	39.63	73.72	22.84	76.47	39.23	77.74	37.64	–	–	75.24	37.35	76.62	47.37	81.06	43.20	70.50	32.15	70.70	36.59
Voxtral-Mini-3B-2507	77.83	36.35	80.53	41.84	–	–	77.39	38.93	78.79	38.36	–	–	–	–	79.95	51.03	–	–	–	–	–	–
Phi-4-multimodal-instruct	79.46	40.01	81.10	**43.53**	–	–	78.57	41.98	**80.20**	**41.29**	–	–	–	–	**81.20**	54.52	–	–	–	–	–	–
Canary-1B-v2	78.32	39.22	80.82	42.74	75.78	25.52	78.52	41.43	79.45	40.03	**70.91**	**31.77**	78.46	41.59	78.26	50.38	83.31	48.78	74.72	39.43	73.71	44.40

Table 15: Per-language COMET (C) and BLEU (B) scores (%) on the **CoVoST2** benchmark.

D EVALUATION: AST (EN→X) PERFORMANCE

	bg		cs		da		de		el		es		et		fi		fr		hr		hu		it	
Model	C	B	C	B	C	B	C	B	C	B	C	B	C	B	C	B	C	B	C	B	C	B	C	B
seamless-m4t-v2-large	87.53	37.01	**86.83**	27.36	**87.06**	41.07	**83.86**	34.40	**84.80**	16.70	81.66	24.40	87.02	23.38	**88.18**	21.03	83.59	**44.81**	**86.67**	**25.48**	**85.51**	**21.60**	83.87	25.28
seamless-m4t-medium	83.32	30.63	80.70	21.65	82.62	34.93	77.69	27.94	80.85	13.82	78.50	21.30	80.11	16.19	80.63	14.18	79.07	37.98	81.36	20.55	78.37	15.69	79.75	21.90
Voxtral-Mini-3B-2507	–	–	–	–	–	–	83.25	31.24	–	–	**82.37**	24.45	–	–	–	–	83.66	41.69	–	–	–	–	83.92	24.83
Phi-4-multimodal-instruct	–	–	–	–	–	–	83.57	**35.57**	–	–	80.90	24.27	–	–	–	–	81.88	39.61	–	–	–	–	81.99	24.39
Canary-1B-v2	**87.73**	**38.14**	86.26	**27.69**	86.89	**41.78**	83.30	33.65	81.49	**23.87**	82.13	**25.67**	**87.32**	**23.54**	87.40	**21.10**	**83.82**	43.42	85.46	24.71	83.94	20.75	**84.12**	**26.82**

	lt		lv		mt		nl		pl		pt		ro		ru		sk		sl		sv		uk	
Model	C	B	C	B	C	B	C	B	C	B	C	B	C	B	C	B	C	B	C	B	C	B	C	B
seamless-m4t-v2-large	**85.42**	20.49	–	–	68.89	**32.45**	84.14	24.61	**84.52**	**18.88**	84.83	43.83	86.41	35.05	**85.18**	**27.55**	**86.40**	**29.04**	**85.91**	24.57	**87.10**	**41.53**	**86.21**	25.55
seamless-m4t-medium	78.96	15.85	–	–	67.57	27.26	80.02	21.44	78.72	14.27	81.97	37.91	81.61	28.76	80.60	22.24	79.73	22.24	78.63	18.65	82.39	34.45	80.66	20.82
Voxtral-Mini-3B-2507	–	–	–	–	–	–	–	–	–	–	84.66	39.74	–	–	–	–	–	–	–	–	–	–	–	–
Phi-4-multimodal-instruct	–	–	–	–	–	–	–	–	–	–	82.65	38.43	–	–	–	–	–	–	–	–	–	–	–	–
Canary-1B-v2	85.13	**21.60**	**86.52**	**29.33**	**69.02**	31.61	**84.25**	**25.81**	83.82	17.98	**85.56**	**44.75**	**87.00**	**36.27**	84.87	27.21	86.21	28.43	84.96	**24.96**	86.43	40.73	85.74	**25.72**

Table 16: Per-language COMET (C) and BLEU (B) scores (%) on the **FLEURS** benchmark (new evaluation).

	de		et		lv		sl		sv	
Model	C	B	C	B	C	B	C	B	C	B
seamless-m4t-v2-large	**81.30**	**37.36**	**82.89**	**29.57**	–	–	**83.10**	**36.53**	**83.34**	**43.71**
seamless-m4t-medium	77.20	32.93	78.52	24.76	–	–	78.80	30.62	79.86	39.46
Voxtral-Mini-3B-2507	76.51	28.78	–	–	–	–	–	–	–	–
Phi-4-multimodal-instruct	79.33	34.12	–	–	–	–	–	–	–	–
Canary-1B-v2	78.37	33.82	80.61	28.09	**81.32**	**27.10**	80.02	31.18	81.12	41.49

Table 17: Per-language COMET (C) and BLEU (B) scores (%) on the **CoVoST2** benchmark.